12-7-2022

Quantifying the Toxicological Effects of the Organic Uv Filters Avobenzone and Homosalate on Acropora Cervicornis

Samantha F. Buckley
Nova Southeastern University

Thesis of
Samantha F. Buckley

Submitted in Partial Fulfillment of the Requirements for the Degree of

Master of Science
Marine Science

Nova Southeastern University
Halmos College of Arts and Sciences

December 2022

Approved:
Thesis Committee

Committee Chair: Dr. D. Abigail Renegar

Committee Member: Dr. Jose V. Lopez

Committee Member: Dr. Nicholas R. Turner

NOVA SOUTHEASTERN UNIVERSITY

HALMOS COLLEGE OF ARTS AND SCIENCES

QUANTIFYING THE TOXICOLOGICAL EFFECTS OF THE ORGANIC UV FILTERS AVOBENZONE AND HOMOSALATE ON *ACROPORA CERVICORNIS*

By

Samantha F. Buckley

Submitted to the Faculty of
Halmos College of Arts and Sciences
in partial fulfillment of the requirements for
the degree of Master of Science with a specialty in:

Marine Science

Nova Southeastern University

December 2022

ABSTRACT

Reports of the environmental effects of organic UV filters such as oxybenzone have led to the marketing of "reef-safe" sunscreen ingredients, including avobenzone and homosalate. Avobenzone provides broad-spectrum UV protection which blocks higher wavelength UV rays, the leading cause of aging and skin cancer. However, as polycyclic aromatic hydrocarbons (PAHs), organic UV filters have similar structures to crude oil and estrogens, some of which have been labeled endocrine disrupters. Common in personal care products, UV filters enter marine ecosystems via wastewater effluent and swimmers. Significant stress and mortality have been observed in juvenile and some adult scleractinian corals after exposure to several UV filters, leading to bans in some coastal regions. This study evaluated the individual effects of avobenzone and homosalate on the Atlantic staghorn coral *Acropora cervicornis* using 96 h assays in a static renewal exposure system. *Acropora cervicornis* exposed to avobenzone exhibited severe responses, including tissue attenuation, reduced growth rates, hypertrophied mucocytes, and mortality with an EC50 of 324.5 µg/L and an LC50 of 407.6 µg/L. *Acropora cervicornis* exposed to homosalate also showed tissue attenuation and hypertrophied mucocytes but to a lesser degree, with an EC10 of 629.9 µg/L. Avobenzone exhibited higher acute toxicity levels to adult coral than the previously banned organic UV filters, including oxybenzone and octinoxate. However, toxicity threshold concentrations were above the estimated solubility of each UV filter and quantified levels detected in coastal waters. Additional research is needed regarding chronic exposure to lower concentrations present in marine environments.

KEYWORDS

Atlantic staghorn coral, sunscreen, acute, toxicity, static renewal exposure assay

ACKNOWLEDGEMENTS

I would like to thank Dr. Denis Dudley, founder of CyberDerm, for funding this project. I would also like to thank my committee members, Dr. Abigail Renegar, Dr. Jose Lopez, and Dr. Nicholas Turner for all their valuable advice and guidance, which made this project possible. Thank you to Kat Meurer, Dawn Bickham, Ellen Skelton, Kyle Pisano, and Eileen Whitemiller of the Marine Toxicology lab for help with coral fragmenting and setting up and running the exposures. Thank you to Dr. Brian Walker for providing support and allowing me the time to step away from work when needed to advance with this project. Many thanks to my former and present coworkers in the GIS and Spatial Ecology lab. Thank you to my boyfriend, Rafael Cobian, for the daily emotional support and even for stepping in to help with buoyancy weights when needed. Lastly, much love and appreciation for all my friends and family who have always supported me and my passions.

TABLE OF CONTENTS

LIST OF FIGURES

LIST OF TABLES

INTRODUCTION

In recent years, attention has been drawn to the possible effects of cosmetic products released into the environment, with particular attention given to ultraviolet (UV) filters. UV filters are present in various personal care products, plastics, fabrics, paints, and textiles (Fent et al. 2010, Mitchelmore et al. 2021). It is undisputed that these compounds are detectable in environments including marine and freshwater ecosystems, sediments, and biota (Wheate 2022, Mitchelmore et al. 2019, Tsui et al. 2017, Bratkovics et al. 2015, Downs et al. 2016), prompting investigation into what impacts may occur in exposed organisms. Danovaro et al. (2008) demonstrated that corals had increased susceptibility to bleaching after exposure to organic UV filters and since then, studies have continued to examine the wide-ranging effects of UV filters on corals. This triggered regions with valuable reef ecosystems, including Palau, US Virgin Islands, Bonaire, Aruba, and Hawaii, to ban all or select organic UV filters from sunscreen products. This has caused a shift in active sunscreen ingredients from oxybenzone to other organic UV filters, such as avobenzone and homosalate, or inorganic (mineral) filters, such as zinc oxide (Sambandan & Ratner 2011). These subsequently have been labeled "reef-safe" without direct evidence confirming these claims (Miller et al. 2021). Although the overall impacts of this exposure are unknown, it is estimated that around 10% of the world's reefs, including approximately 40% of coral reefs along coastal areas, are at risk of exposure to UV filters (Downs et al. 2016).

Organic UV filters in sunscreens

Sunscreens are formulated to effectively block ultraviolet radiation (UVR) from coming in direct contact with our skin. Ultraviolet radiation is classified into three groups from longest to shortest wavelength: UVA, UVB, and UVC. Approximately 80-90% of UVA rays (UVA1 400-340nm, UVA2 340-320) reach the Earth's surface, while only 1-10% of UVB rays (320-290nm) can penetrate the Earth's atmosphere (Raffa et al. 2018). UVA and UVB rays interact with living tissues, resulting in biochemical and physiological changes (Staberg et al. 1983, Setlow et al. 1993, Nurayanan et al. 2010, American Cancer Society 2019). This commonly results in sunburn, photocarcinogenesis, immunosuppression, and photoaging in humans. The two forms of UVR react with the skin differently based on their varying wavelengths. UVB rays, with a shorter wavelength, penetrate the epidermal layer of skin, resulting in structural DNA damage and are the main driving factor of sunburn for this reason. On the other hand, UVA rays penetrate deeper into

the dermis layer and cause indirect DNA damage through the formation of reactive oxygen species, which then cause breaks in the DNA's tertiary structure. While both forms can result in cancer, UVA (more significantly UVA1) radiation is the primary cause of skin cancer (Stiller et al. 2019).

Sunscreens are typically purchased based on the sun protection factor (SPF) displayed on the container. The SPF, also known as the sunburn protection factor, is measured based on the product's ability to block the UV radiation that causes sunburn (Wang et al. 2011). Since sunburn is primarily driven by shorter wavelength rays (UVB and UVA2), the measurement of a sunscreen's SPF is based on the product's ability to block these two specific wavelength groups (Sambandan et al. 2011). Most approved UV filters in sunscreens are more effective at blocking UVB rays, leading to a higher presence of UVB-biased sunscreens which are less effective at blocking the longer UVA1 rays. Based on this information alone, it is apparent that much more research is needed to ensure sunscreen products contain the most effective active ingredients. Skin cancer rates are still steadily increasing; the incidence rate of melanoma has increased by around 3% each year from 2006 to 2015 in adults over the age of 50 years (American Cancer Society 2019).

UV filters can be separated into organic (e.g., oxybenzone and avobenzone) and inorganic or mineral (e.g., zinc oxide and titanium dioxide). The inorganic filters block UVR using a physical barrier. These effectively block broad-spectrum UV radiation, spanning both UVA and UVB rays. A downside to inorganic filters is that a thick application is required, and a white coating is often left visible. On the other hand, organic UV filters are aromatic compounds that absorb UVR and convert it into heat energy. They are typically specified for blocking a smaller range of the UVR spectrum (Siller et al. 2019). There are currently 16 FDA-approved organic UV filters (Sambandan et al. 2011). The most frequently used include avobenzone, oxybenzone (BP-3), homosalate, octisalate (EHS), octocrylene (OC), octinoxate (EHMC), ecamsule (TDSA) and enzacamene (4-MBC), a majority of which block the UVB and UVA2 range that leads to sunburn. Only a few, such as avobenzone and ecamsule, are effective at blocking the deeper penetrating UVA1 rays (Siller et al. 2019). Avobenzone is the only UV filter able to protect against rays with wavelengths as high as 400nm. However, it is a volatile compound whose photoprotective properties begin to diminish after a certain amount of sun exposure. In contrast, homosalate is a very stable compound,

and when added as a second ingredient, it stabilizes avobenzone, thus why avobenzone and homosalate are commonly paired (Sambandan and Ratner 2011).

Composition and toxic effects of organic UV filters

Organic UV filters are polycyclic aromatic hydrocarbons, a class of organic compounds consisting of two or more aromatic rings or benzene rings (Figure 1). These compounds have similar structures to crude oil and estrogens, allowing them to disrupt cellular and hormonal processes (Schlumpf et al. 2001). Furthermore, the small molecular weight of these organic UV filters (< 500 Daltons) allows transdermal absorption in human skin. This calls into question the effects of these compounds on the human body, especially considering cases where these products are applied daily. The amount of each active ingredient in various products can be as high as 15%, leading to exposure quantities of grams per day (Wang et al. 2019). A 2008 CDC study found that 97% of roughly 2,500 participants had BP-3 detected in urine samples (Calafat et al. 2008). These compounds have also been quantified in blood, urine, breast milk, and amniotic fluid (Schneider et al. 2018).

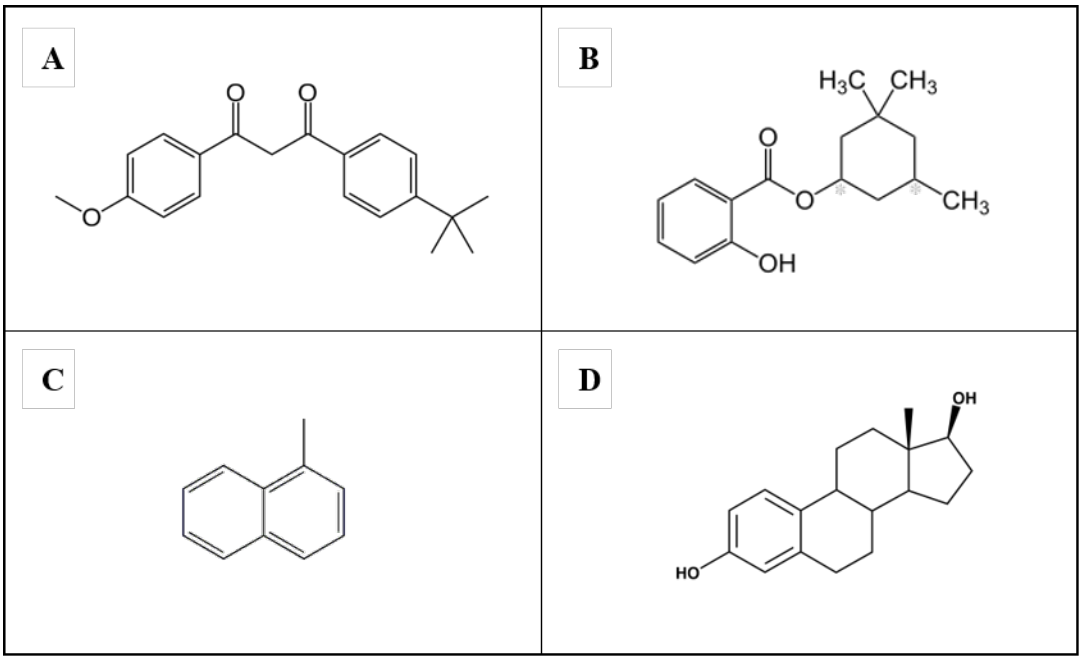

Figure 1. Chemical structure of (**A**) avobenzone, (**B**) homosalate, (**C**) the petroleum hydrocarbon 1-methylnaphthalene, and (**D**) 17 b-estradiol.

The FDA regulates UV filters since they are classified as over-the-counter (OTC) products in the United States. In 2016, the FDA released an update requesting an assessment of the human systemic absorption of sunscreen ingredients, stating that any compounds with systemic absorption of greater than 0.5 ng/ml would need further testing to understand the effects (Wang et al. 2019). In a recent maximum usage trial where commercial sunscreens, including the UV filters avobenzone, BP-3, OC, and TDSA were applied four times per day for four days (covering 75% of the body), the blood plasma concentrations of all participants exceeded the 0.5ng/ml limit; and these compounds were present in the blood for up to three days after the last application (Matta et al. 2019). In a subsequent study, which added homosalate, EHS, and EHMC, they also observed concentrations that surpassed the FDA threshold on day one after just a single application (Matta et al. 2020). These studies confirmed the need for additional research into the clinical significance of these results.

Past research on the cellular and hormonal disruption level of UV filters has shown that BP-3, homosalate, 4-MBC, and a few others increased cell proliferation of cultured MCF-7 breast cancer cells (Schlumpf et al. 2001). The same study showed that 4-MBC and EHMC applied topically and administered orally to rats led to an increase in uterine weight. However, predictive models indicate that it would take anywhere from 35-277 years of daily application (depending on the application amount) for a human body to incur the effects seen in rat models (Wang et al. 2011, Schneider et al. 2018). However, further studies have labeled organic UV filters as estrogen agonists, androgen antagonists, progesterone antagonists, and others (Klimova et al. 2013, Oral et al. 2020). Additionally, there is evidence of an increased incidence of melanoma from the use of sunscreen particularly in areas of latitudes greater than 40º (Gorham et al. 2007, Ngoc et al. 2019). As UV filters absorb UVB radiation, they can transmit UVA, leading to a risk of cancer formation. While some percentage of these compounds may be retained in tissues, they eventually leave the human body through various pathways and thus are likely to eventually end up in the oceans.

Organic UV filters in marine environments

There are two main inputs of UV filters to coastal waters. One source is directly from swimmers, as people are likely to apply sunscreen products at the beach. Another is in wastewater effluent, as the chemical properties of organic UV filters make it difficult for them to be entirely removed during wastewater treatment (Shneider and Lim 2019). In Brazil and Switzerland,

wastewater influent and effluent testing demonstrated that UV filters, including BP-3, 4-MBC, and EHMC, remained in the treated water at 18 ng/L to 2.7 µg/L (Balmer et al. 2005, da Silva et al. 2015). The exact amount of sunscreen compounds that enter the ocean is unknown, with some studies estimating 4,000 – 6,000 tons and others estimating up to 20,000 tons of sunscreen each year (Danovaro et al. 2008, Corinaldesi, 2001). In most cases, the amount of UV filters quantified in coastal ocean water averages around 100 ng/L; however, there is high variability between studies (Mitchelmore et al. 2021). UV filters to have been quantified at levels above 1000 ng/l include BP-3, EHMC, OC, and homosalate (Tashiro and Kameda, 2013, Tsui et al. 2014, Bargar et al. 2015). Only one study found BP-3 at levels above 1,000,000 ng/L (1 mg/L) (Downs et al. 2016).

Of all the organic UV filters, BP-3 has been tested the greatest number of times in studies quantifying sunscreen compounds in seawater and has a detection frequency of 76% (Mitchelmore et al. 2021). BP-3 was present at the highest levels in the U.S. Virgin Islands, ranging from 75 ppb (ug/L) to 1.4 ppm (mg/L) in areas with frequent swimmers (Downs et al. 2016). It was also observed in coastal waters around South Carolina (37.6-591ng/L), China (12.9 - 5429 ng/L), Japan (0.5-1340 ng/L), Hawaii (5 - 19.2 ug/L), Palau (4.12 – 18.5 ng/L), and the Arctic (17 – 33 ng/L) (Tashiro and Kameda, 2013, Tsui et al. 2014, Bratkovics et al. 2015, Downs et al. 2016, Bell et al. 2017, Tsui et al. 2017, Wood 2018, Mitchelmore et al. 2019). Further research has shown that the half-life of BP-3 in seawater is several months. However, the nearly constant renewal makes it a persistent contaminant (Vione et al. 2013).

Other commonly used UV filters have also been observed in coastal waters. OC had an even higher detection frequency (85%) than oxybenzone (Mitchelmore et al. 2021). OC has been found in the U.S. Virgin Islands, South Carolina, Japan, China, New York, California, and the Arctic at concentrations from 26 to 6,812 ng/L (Tashiro et al. 2013, Tashiro and Kameda, 2013, Tsui et al. 2014, Bratkovics et al. 2015). EHMC has also been quantified frequently and at high levels in the same regions ranging from 25 to 4,043 ng/L (Bargar et al. 2013, Tsui et al. 2014, Bratkovics et al. 2015). Homosalate has an average detection rate of 74% and has been quantified in Japan, China, New York, California, Hawaii, and the U.S. Virgin Islands, at levels ranging from 0.5 to 2,812 ng/L (Bargar et al. 2013, Mitchelmore et al. 2019, Tashiro et al. 2013, Tsui et al. 2014). Fewer studies have investigated avobenzone and detection frequencies ranging from 0% to 97% (Mitchelmore et al. 2021, Tsui et al. 2014). Avobenzone was quantified in South Carolina,

China, Japan, New York, California, and the Arctic up to 721 ng/L, however no detectable levels were found in Hawaii (Tsui et al. 2014, Bratkovics et al. 2015, Mitchelmore et al. 2019). Many of these studies also confirm that the concentrations are higher closer to shore while decreasing further offshore and are higher during peak tourist seasons and at certain times of day (Bratkovics et al. 2015, Bargar et al. 2013).

UV filters generally have high octanol-water partitioning coefficients (K_{OW}), with values between 4 and 8, indicating that they are lipophilic. This is a vital attribute for sunscreen products since, to be effective, they must absorb into the skin instead of washing off upon contact with water (Wheate 2022). Once released into the environment, these compounds have a high affinity to particulate organic matter, e.g., sediments and tissues of organisms (Bratkovics et al. 2015). Measurable concentrations of UV filters are found in the sediments of nearshore reefs and coral tissues (Tsui et al. 2017, Mitchelmore et al. 2019). The median detection levels of UV filters, such as BP-3, EHMC, OC, avobenzone, and homosalate, range from 0.05 to 19.5 ng/g in sediments and 8.3 to 341 ng/g in coral tissues. These compounds have also been quantified in the tissues of other marine species, including bivalves, fish, and cetaceans (Wheate 2022, Sang et al. 2016, Gago-Ferrero et al. 2013).

Coral reefs

Coral reef ecosystems are some of Earth's most valuable and diverse regions, with estimates of biodiversity in the millions of species worldwide (Reaka-Kudla, 1997, Fisher et al. 2015). Beyond their incredible diversity, coral reefs also provide vital services, including protecting coastlines from erosion, providing millions of dollars in revenue and jobs in the forms of tourism and recreation, supporting fisheries as they are nursery habitats for many species, and allowing research into new pharmaceuticals (Richmond 1993, Moberg and Folke 1999). The main engineering species of coral reef systems are scleractinian or stony corals. Stony corals survive in clear, tropical, oligotrophic environments using their relationship with unicellular dinoflagellates (Symbiodiniaceae). Through photosynthesis, these algal symbionts provide the coral host with most of their metabolic requirements (Iluz and Dubinsky 2015). This relationship between the coral host and algal symbiont acts as the initial trophic link in coral reef ecosystems by means of carbon fixation (Richmond 1993).

Unfortunately, more than ever, corals face immense environmental stress due to anthropogenic factors. Stressors such as climate change, global warming, ocean acidification, pollution, disease, overfishing, and coastal development are some of the factors which cause coral bleaching and mortality. Ecological extinction is predicted within the next 20 - 50 years if corals are unable to adapt and effective management is not implemented (Louis et al. 2017). On a global scale, ocean warming is believed to generate the most significant negative impact on corals (Fel et al. 2019). However, reef ecosystems in areas with high populations and high tourism traffic are exposed to additional stressors in the form of pollution from sewage runoff and people directly around and in the water (Danovaro et al. 2008; Downs et al. 2014; McCoshum et al. 2016). Coastal regions are among the most populated areas, with roughly 40% of the world's population living within 60 miles of the coast; a number that is expected to increase in the next century (Wood 2018).

Toxicity of organic UV filter to corals

Research into the effects of organic UV filters on coastal marine life is new, and currently only ten publications demonstrate their effects on stony corals. These studies have included 17 organic UV filters and 5 different species of stony coral, mostly Indo-Pacific branching corals, at either juvenile or adult phases. Results provide evidence of the role of UV filters as endocrine disrupters with direct effects, including physical deformities in juvenile corals (Downs et al. 2016). Corals at varying life stages were shown to have an increased susceptibility to bleaching when exposed to UV filters (Danovaro et al. 2008, Downs et al. 2016). Subsequent studies on corals then confirmed a suite of additional effects on corals, including mortality, polyp retraction, photosynthetic efficiency, algal density, growth, settlement, and the microbiome (Johnsen, 2018, Fel et al. 2019, He et al. 2019a, Wijgerde et al. 2020).

Danovaro et al. (2008) was among the first to investigate coral response to UV filter exposure, testing brand-name sunscreen products and individual ingredients by enclosing coral fragments in polyethylene bags and incubating them *in situ*. Danovaro et al. (2008) concluded that sunscreens (with organic UV filters) induce the lytic cycle in the zooxanthellae resulting in bleaching of the coral; all sunscreen brands tested, and four out of the seven individual ingredients resulted in complete bleaching. Increased viral abundance in the seawater surrounding the coral samples (by a factor of 15 compared to controls) was also observed after adding sunscreen. Downs et al. (2016) notably drove the BP-3 ban in Hawaii, as data from this study supported the suggestion

that BP-3 is a skeletal endocrine disrupter. This was confirmed with observations of the ossification of *Stylophora pistillata* planulae; planulae exposed to 22.8 µg/L developed deformations, lack of ciliary movement, bleaching, and mortality. Other effects included increases in DNA abasic sites and the percentage of dead coral cells.

Most studies are performed *ex-situ* as it is easier to control the concentrations and exposure times of the experiment. The lowest effect concentration observed was a 24-h 50% effect concentration (EC50) of 49 µg/L of BP-3 which caused deformities in *Stylophora pistillata* planula (Downs et al. 2016). Four studies have investigated the effects of BP-3 on corals, with common observations of polyp retraction, bleaching, and reduced algal density. The lowest observed effect concentration (LOECs) for juvenile corals was 2.28 µg/L after 8 h. For adult corals, a LOEC of 10 µg/L after 7 d was observed for polyp retraction and greater than or equal to 1000 µg/L for more severe effects such as bleaching and mortality (Downs et al. 2016, He et al. 2019a). Other benzophenone UV filters, including benzophenone-1 (BP-1), benzophenone-2 (BP-2), benzophenone-4 (BP-4), and benzophenone-8 (BP-8), have also been investigated, and BP-8 and BP-1 appeared more toxic to corals than BP-3 (He et al. 2019a). UV filters such as EHMC, OC, and EHS exhibited LOECs of 1000 µg/L or greater in adult coral studies (He et al. 2019b). However, in many of these studies, nominal concentrations only were used, and measured concentrations are likely much lower due to the low solubility of these compounds. One study analytically confirmed exposure concentrations and found, based on photosynthetic efficiency, a LOEC of 519 µg/L for OC and a LOEC of 87 µg/L for avobenzone after a chronic 35 d exposure. All *ex-situ* studies of UV filter effects on coral species are summarized in Table A1.

Only two studies have attempted *in situ* exposures, including Danovaro et al. (2008). Adult corals exhibited bleaching at a low concentration of 33 µl/L from the UV filters: butylparaben, EHMC, BP-3, and 4-MBC. No effects were seen from avobenzone, OC, or EHS; however, concentrations were provided as the volume of active ingredients and not mass to volume. A second *in situ* study tested whether a commercial sunscreen brand (Banana Boat SPF 50) would affect *Pocillopora* corals off Pichilingue, Baja California Sur by expelling solutions of the sunscreen in water onto the coral fragments three times over the course of a day (Skelly et al. 2012). Bleaching was observed, but this was attributed to the exposure method instead of the UV

filters, as there were no significant treatment effects. The UV filters used in the sunscreen brand at that time were not listed in the study. These two studies are summarized in Table A2.

The toxic effects of organic UV filters have also been observed in algae, flatworms, anemones, and fish. One test on the algae *Isochrysis galbana* found significant growth effects after exposure to BP-3 and EHMC with 72-h EC50s of 13.87 µg/L and 74.73 µg/L, respectively (Paredes et al. 2014). Decreased sexual reproduction in flatworms and significant behavioral stress responses in anemones were seen when exposed to 0.026 ml/ L and 0.26 ml/L, respectively, of Equate sunscreen (13% homosalate, 6% BP-3, 5% OC, 5% EHS, and 3% avobenzone) (McCoshum et al. 2016). Effects on fish species include malformations, altered swimming behavior, reduced growth, and mortality with a 96-h EC50 of 0.372 mg/L 4-MBC for *Solea senegalensis* larvae and a 96-h 25% lethal concentration (LC25) of adult *Amphiprion ocellaris* at 100 mg/L BP-3 (Araújo et al. 2018, Barone et al. 2019).

STATEMENT OF RESEARCH

Unlike the more commonly studied UV filters such as BP-3, OC, and EHMC, research on the human and environmental impacts of avobenzone and homosalate is lacking. Both have been observed to absorb into the skin and be present in the blood, urine, and breast milk, like the more well-studied UV filters. The few studies investigating the effects of avobenzone on corals have shown a decrease in photosynthetic efficiency along with no visible bleaching (Danovaro et al. 2008, Fel et al. 2019). Additionally, avobenzone has been seen to cause immobilization and decreased reproduction in planktonic organisms and flatworms (Park et al. 2017, McCoshum et al. 2016). Very few studies exist on the impact of homosalate on corals or other marine organisms. Only one study observed polyp retraction after exposure to 1000 µg/L of homosalate after 7 d (Stien et al. 2020)

In much of the previous research considering the potential toxicological effects of UV filters, there is high procedural variability with inconsistent methodology, lengths of exposures, coral species/life stage, and lack of effect concentrations. This variability adds complexity when comparing and validating results. For example, organic UV filters have very low solubilities, thus maintaining consistent concentrations in aquatic exposure tests is challenging. For this reason, these compounds must be first dissolved in a solvent to generate aquatic concentrations required

for toxicity testing; solvents used have included methanol, propylene glycol, and dimethyl sulfoxide (DMSO). Solvents, such as DMSO, can increase the biological uptake of a test substance and thus may inflate observed effects (Kais et al. 2013, Mitchelmore et al. 2021). Using solvents requires both a negative control (seawater) and solvent control (seawater and solvent) to account for any unintended solvent-induced effects, and solvent controls were not employed in previous studies. Adequate analytical characterization of test exposure media is also frequently lacking. The studies previously described used nominal concentrations to calculate threshold EC50 values without measuring the experimental exposure levels and confirming the bioavailability to the test organism. As the exposure concentrations were not measured, it is possible that threshold values were over or underestimated.

To provide new information on the effects of avobenzone and homosalate exposure on scleractinian corals, this study tested the effects of these two UV filters on the ESA-endangered Atlantic staghorn coral *Acropora cervicornis*. Specifically, whether the compounds elicit visible stress responses in *A. cervicornis* and the level of physiological damage present following the exposure. Coral health was assessed at multiple levels, including coral condition, growth, photosynthetic efficiency, and cellular tissue health. The hypotheses tested can be found in Table 1. Ninety-six-hour exposures were completed in a closed static renewal system. Effect concentrations were determined based on subacute effects (e.g., coral condition) and acute effects (mortality).

Table 1: Hypotheses and associated analytical methods used in this study.

	Null Hypothesis	Analytical Method
H_0 1	Avobenzone has no effect on the visual appearance of *Acropora cervicornis* Homosalate has no effect on the visual appearance of *Acropora cervicornis.*	Semi-quantitative scoring system
H_0 2	Avobenzone has no effect on the photosynthetic efficiency of the symbionts of *Acropora cervicornis.* Homosalate has no effect on the photosynthetic efficiency of the symbionts of *Acropora cervicornis.*	Pulse amplitude modulation (PAM) Fluorometry
H_0 3	Avobenzone has no effect on the calcification of *Acropora cervicornis* Homosalate has no effect on the calcification of *Acropora cervicornis.*	Buoyant wet weight determination
H_0 4	Avobenzone has no effect on the cellular and tissue health of *Acropora cervicornis.* Homosalate has no effect on the cellular and tissue health of *Acropora cervicornis.*	Histological analysis

METHODOLOGY

Organism collection

The coral species used for this study, *Acropora cervicornis,* is a shallow water branching coral local to southeast Florida. This species was chosen based on its sensitivity to environmental contaminants, while its shape and rapid growth are suitable for experiments involving fragmentation and observation (Greer et al. 2009, Turner 2020). Tips of *A. cervicornis* branches were collected from established colonies at the Nova Southeastern University's Onshore Coral Nursery. Fragments were trimmed into 3-4 cm branch tips and attached to labeled aragonite tiles (3 cm x 3 cm, 0.25 cm thickness) using a small amount of cyanoacrylate gel glue (Loctite Super Glue). The coral fragments were acclimated in an 1100-liter indoor recirculating system for 2-4 weeks prior to the exposures. The system was maintained at 26 °C with a salinity of 35 ppt (artificial seawater prepared with reverse osmosis water and Tropic Marin Classic Sea salt) with water motion provided by powerheads (Hydor Koralia 3G circulation and wave pump) and a wave maker (Tunze Comline Wavebox 6214). Ecotech Radion G4 Pro LED lights were programmed to mimic sunrise and sunset with a photoperiod of 12 h. Throughout the acclimation period, corals were fed coral-specific dissolved nutrients (Brightwell Coral Amino) three times per week.

Avobenzone / homosalate dosing

Avobenzone (Pharmaceutical secondary standard certified reference material CAS: 70356-09-1, Sigma Aldrich, purity>99%) and homosalate (Pharmaceutical secondary standard certified reference material CAS 118-56-9, Sigma Aldrich, purity>99%) stock solutions were prepared by dissolving weighed amounts of each UV filter in methanol (Fisher Scientific, HPLC Grade) in volumetric flasks. Avobenzone and homosalate have low solubilities (0.027 mg/L and 0.5 mg/L, respectively) and high octanol/water partition coefficients, Log Kow, (6.1 and 6.34, respectively) (Mitchelmore et al. 2021). Dissolution of the UV filters in methanol allowed for higher solubilization of these lipophilic compounds in seawater.

For avobenzone, nominal concentrations were chosen based on values from Fel et al. (2019). A 25 mg/ml primary stock in methanol underwent variable dilutions to create the four working stock solutions (Table 2). Exposure media was made by adding 120 µl of each working stock to 3 L of seawater to create concentrations of 125 µg/l, 250 µg/l, 500 µg/l, and 1000 µg/l.

Table 2: Stock solutions for avobenzone exposure (mg/L).

Primary Stock	Working Stock	Exposure media
25 mg/ml	3.125	0.125
	6.250	0.250
	12.500	0.500
	25.000	1.000

As there are no previous analytically confirmed exposure studies with homosalate in corals, a 48 h 5400 µg/l range-finding exposure was performed with a single concentration of 5400 µg/l in a beaker with two *A. cervicornis* fragments. This concentration was chosen as it is a ten-fold increase from the solubility of homosalate, thus allowing the highest possible amount of solubilized material. After 48 h, there was no visible stress response from the coral fragments, so 5400 µg/l was chosen as the highest exposure concentration. A 100 mg/ml primary stock in methanol underwent variable dilutions to create the four working stock solutions (Table 3). Exposure media was made by adding 300 µl of each working stock to 3 L of seawater to create concentrations of 5400 µg/l, 1800 µg/l, 600 µg/l, and 200 µg/l.

Table 3: Stock solutions for homosalate exposure (mg/L).

Primary Stock	Working Stock	Exposure media
100 mg/ml	2	0.200
	6	0.600
	18	1.800
	54	5.400

Exposures

Avobenzone and homosalate 96 h exposures were completed separately in a static renewal exposure system in the NSU Marine Toxicology laboratory at the Guy Harvey Oceanographic Center (Figure 2). Seawater from the acclimation system was filtered to 1 µm for use in the exposure system. Lighting was the same as the acclimation system (Ecotech Radion LED lights programmed to a photoperiod of 12 h); the corals were not directly fed during the exposures. Each exposure included four replicates of each nominal concentration, MeOH/seawater controls, and seawater controls for a total of 24 test chambers. Exposure media was made in 5000 ml glass media bottles and transferred into each replicate chamber (1.5 L each). For the methanol/seawater controls, 1.5 L of filtered seawater was added to each chamber, then 60 µl (40 µl/L) and 150 µl (100 µl/L) of methanol (representative of the highest MeOH concentration in the exposure treatments) were added for the avobenzone and homosalate exposures, respectively. Two coral fragments were randomly assigned to each exposure chamber.

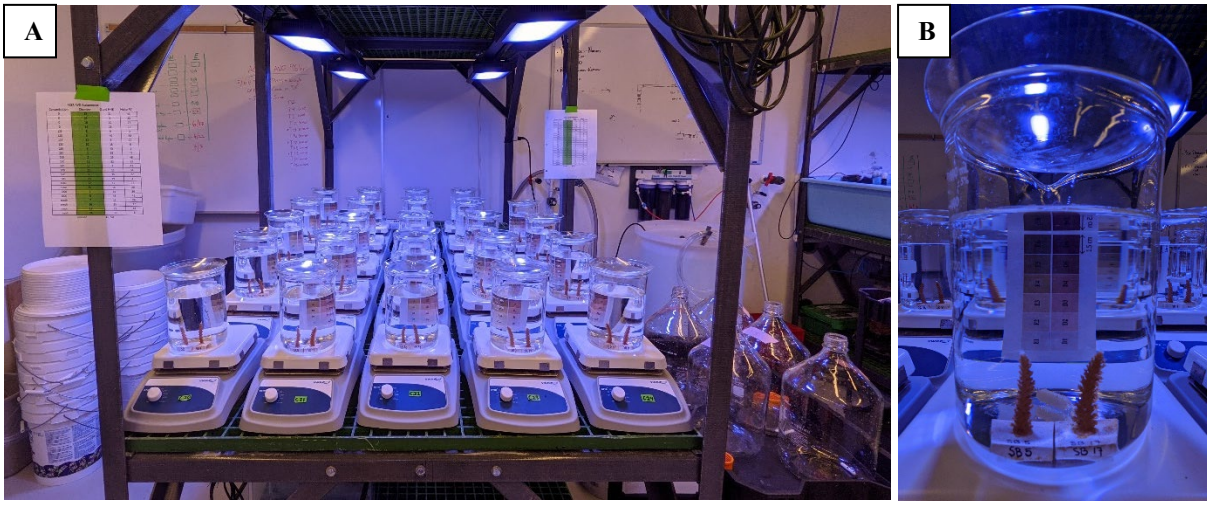

Figure 2. (**A**) Static renewal exposure system using 1.5L glass beakers with Teflon-coated magnetic stir bars on stir plates. (**B**) Beakers were covered with watch glasses to prevent evaporation.

Test solutions were renewed every 24 h. New stock solutions were prepared daily, and water renewals were completed one treatment at a time in order of increasing treatment concentration (e.g., seawater control, MeOH/sweater control, lowest to the highest concentration of UV filter). Corals were removed from the chambers and briefly placed in a temporary holding container while the exposure chambers were emptied and refilled.

At the end of the 96 h exposure, one *A. cervicornis* fragment from each chamber was processed for further analysis, and the other was placed back in the acclimation system for post-exposure observation. Coral fragments were maintained under the same conditions as during the pre-exposure acclimation period. In the case of mortality of one or both fragments in one chamber, the one with the most living tissue was chosen for processing.

Water quality and chemical analysis

Water quality samples were collected from each chamber at the end of the 96 h exposures. Temperature, pH, and dissolved oxygen (DO) were measured with a YSI 556 Multiprobe System. Phosphate (PO_4), ammonia (NH_3), nitrite (NO_2), and nitrate (NO_3) levels were analyzed with a HACH DR850 colorimeter. Alkalinity was determined by potentiometric titration with a Mettler-Toledo DL22 autotitrator. For analytical verification of exposure concentrations, duplicate 10 ml samples were collected throughout the avobenzone and homosalate exposures in 20-ml amber VOA vials (Thermo Fisher Scientific, I-Chem certified). Samples were taken from each exposure stock solution at the start of the exposure, before and after each 24 h water change, and at the end of the exposure. Homosalate water samples also underwent a hexane extraction and were transferred to ASV vials. Water samples from both exposures were shipped to the University of Maryland Center for Environmental Science for analysis.

Evaluation of corals

The coral fragments were visually evaluated based on five different metrics to obtain a broad understanding of the effects of avobenzone and homosalate on *A. cervicornis*. These metrics have been used in previous studies investigating coral responses to environmental contaminants (Renegar and Turner 2021, Meurer 2022).

Coral condition and mortality

Coral condition in this study is defined as visible physiological stress responses of the coral. The physical condition of the coral was evaluated throughout the exposure using a semi-quantitative scoring metric ranging from 0 (normal) to 3 (maximum effect) (Table 4). Scoring metrics included coloration, polyp retraction, tissue swelling, tissue attenuation, and mucous production. Based on a histologically verified stress index developed for real-time coral health assessment, this scoring system has been utilized consistently in NSU's Marine Toxicology lab (Renegar and Turner 2021, Meurer 2022). Scores were determined through visual observations with an estimated precision level of 0.5. Throughout each exposure, scores were recorded every 4 h for the first 12 h, then every 12 h for the remainder of the 96 h. Digital photographs were taken at each scoring time point. A single percent effect for each coral fragment at each time point was calculated by summing individual scores for each metric and dividing by the total maximum score. The percent effect of each replicate fragment was then averaged to determine a single percent effect for each chamber.

Table 4: Criteria for qualitative scoring coral condition characteristics (Renegar and Turner 2021).

Range	Diagnostic criteria
0-normal	Color: appears normal Polyps: fully extended or loosely retracted Mucus: normal mucus production Tissue: no tissue swelling, no mesenterial filaments
1-mild	Color: slight lightening of coloration Polyps: retracted and slightly closed Mucus: normal to slightly elevated Tissue: slight coenenchyme swelling and/or polyp distension
2-moderate	Color: moderate lightening of color Polyps: evident polyp retraction with full polyp closure Mucus: moderately elevated mucus production Tissue: moderate coenenchyme swelling and/or polyp distension
3-severe	Color: significant lightening of coloration, bleaching Polyps: polyps tightly retracted and skeletal ridges exposed Mucus: mucus sheets evident Tissue: severe coenenchyme swelling and/or polyp distension

Percent tissue mortality was also estimated throughout the exposure. Mortality was defined similarly to Turner et al. (2020) by "severe tissue attenuation to the point of skeletal element exposure," from which percent mortality scores were assigned, with a resolution of 5%. The percent mortality of each replicate fragment was then averaged to determine a single value for each chamber. In addition, 1 wk post-exposure mortality percentages were recorded.

Photosynthetic efficiency

The photosynthetic efficiency of the algal endosymbionts was measured with a pulse amplitude modulated fluorometer (Diving-PAM, Walz, Germany). Measurements were recorded at the start and end points of the exposure and at 1 wk post-exposure to quantify recovery. Changes in endosymbiont efficiency can signal disruption to the coral-algal symbiont relationship, resulting in coral bleaching. The Diving-PAM quantifies photosynthetic efficiency by measuring the maximum quantum yield (F_m-F_o/F_m) of the algal symbionts by applying a saturation pulse of light and determining yield from the ratio of initial fluorescence ($F_{o)}$ to maximum fluorescence (F_m). Before measuring, all corals were pre-adapted in the darkness for at least 1 h, and the lights remained off for the duration of the measurements. The following parameters were chosen to determine yield for *A. cervicornis*: measuring light intensity = 5, damping = 2, gain = 4, saturation intensity = 8, and saturation width = 0.8. The accuracy of these settings was confirmed by verifying that the saturation curve displayed the characteristic plateau required for accurate readings. The fiber optic sensor was held perpendicular to the middle of the fragment, and its distance was adjusted to obtain initial fluorescence readings of 130-250. If partial mortality of the fragment was present and an initial fluorescence reading of 130 was not reached, that data point was not reliable and was removed. Two measurements were taken at opposite sides (around the circumference) of the middle of the fragment, which were averaged to provide a maximum yield for each fragment. The average maximum yield of each replicate fragment was then averaged to determine a single reading for each chamber. In the post-exposure readings, only one coral fragment per chamber remained, so the average of the two measurements for each coral represented the reading for each chamber.

Calcification

Calcification was used to estimate any change in the growth rates of the *A. cervicornis* fragments. Calcification was quantified using buoyant wet weight, a common practice to measure

short-term coral growth rates (Davies 1989). Weights were recorded at the start and end points of the exposure and were repeated one-week post-exposure to quantify recovery. Additionally, buoyant wet weights were recorded during the acclimation period (over 1 wk pre-exposure) for the homosalate test to provide baseline growth rates. Calcification rates (growth rates) were calculated by converting wet weights to air weights, then dividing the change in growth by the number of days to get a percent change per day (Turner 2020). In any instance of a negative growth rate, that value was replaced with zero.

Cellular and tissue health

Samples for histological analysis were fixed at the end of the exposures. Coral fragments were stored in glutaraldehyde fixative solution [2 mL of 70% glutaraldehyde in 68 mL of cacodylic buffer (2.16 g cacodylic acid in 200 mL of .22 µm filtered seawater)] and kept at 4°C for 4-6 days. Decalcification was performed in 5% hydrochloric acid (HCl)/ethylenediaminetetraacetic acid (EDTA) in a seawater solution. Samples were dehydrated in a series of ethanols and xylene, then embedded in paraffin and sectioned at 5 µm in longitudinal and transverse sections. Sections were mounted on slides with 2 replicate sections on three replicate slides per fragment, then deparaffinized with xylene and stained following the Harris's hematoxylin and eosin (H&E) protocol. Slides were viewed and photographed under an Olympus BX 43 light microscope.

Histology samples were scored using a semi-quantitative scale developed by Miller et al. (2014) and modified by Dr. Esther Peters, Morgan Hightshoe, and Megan Bock (Hightshoe 2018 and Bock 2018) (Table A3). Cellular changes were assessed and rated (0 = Within Normal Limits, to 5 = Severe). Areas of observation included epidermal mucocytes (EM), costal tissue loss (CTL), zooxanthellae in the surface body wall (ZSBW), cnidoglandular band epidermal mucocytes (CBEM), cnidoglandular band degeneration (CB), cell dissociation of mesenterial filaments (MF), gastrodermal architecture (GA), and calicodermis (C). Averages for each of the eight scored parameters and total scores (sum of all parameters) were used to investigate treatment effects. The proportion of the maximum score possible, calculated from total scores, was then used to determine threshold concentrations.

Statistical analysis

Statistical analysis was completed with R statistical software (Version 4.1.0). All data collected were checked for normality (Shapiro-Wilk) and homoscedasticity (Bartlett/Levene). If data did not meet normality assumptions, transformations were completed where possible, or non-parametric tests were used. The seawater and methanol controls were averaged and pooled to test for treatment effects after confirming that no statistically significant difference existed between the control groups. A non-parametric Kruskal-Wallis test (α=0.05) on ranks of untransformed data was used to compare mean coral condition scores, mortality, growth rate (homosalate exposure), and total histological scores (avobenzone exposure). Significant treatment effects seen in non-parametric data were further analyzed with the post hoc Mann-Whitney U-test. A parametric one-way ANOVA (α=0.05) was used to compare photosynthetic yield, growth rates (avobenzone exposure), and total histological scores (homosalate exposure). Dunnett's post hoc test analyzed significant treatment effects in parametric data. Non-parametric methods were used for the histological parameters including CTL, CBEM, GA (homosalate exposure), and C (homosalate exposure). Parametric methods were used for the histological parameters including EM, ZSBW, CB, MF, GA (avobenzone exposure), and C (avobenzone exposure). For all water quality parameters, non-parametric methods were used to analyze temperature, pH (avobenzone exposure), alkalinity (homosalate exposure), and all nutrients. Parametric methods were used to analyze pH (homosalate exposure), dissolved oxygen, and alkalinity (avobenzone exposure). Parametric post hoc tests for water quality parameters were completed with Tukey's test and non-parametric post hoc tests were completed with the Multiple comparisons test.

Sublethal and lethal threshold concentrations were determined with the *drc* package in R statistical software. Scored metrics, including coral condition (Table 4), histological analysis (Table A3), and mortality, were converted to the percent of the total score possible to calculate 50% effect concentrations (EC50) and 50% lethal concentrations (LC50). Photosynthetic yield and calcification rates were normalized to baseline measurements to determine the 50% inhibition concentration (IC50). As no baseline growth rates were recorded during the avobenzone exposure, results from the treatment groups were normalized to the average control growth rate. Sublethal concentrations (EC50) of avobenzone and homosalate were calculated using a log-logistic 4-parameter dose-response model with a maximum effect fixed at 1 (Renegar and Turner 2021,

Turner et al. 2021). Lethal concentrations (LC50) were calculated with a minimum effect fixed at 0 and a maximum effect fixed at 1. Additionally, no observed effect concentrations (NOEC) and lowest observed effect concentrations (LOEC) were determined based on significant treatment effects.

RESULTS FROM EXPERIMENT 1 (AVOBENZONE)

Water quality

Mean water quality parameters at the end of the 96-h exposure are summarized in Table 5. A significant difference in pH between treatments was found, (Kruskal Wallis, $p=0.009$), and post-hoc analysis showed significantly higher values in the 250 µg/L and 500 µg/L treatments compared to the pooled controls (Multiple comparisons, $p=0.006$ and $p=0.01$, respectively). There was no significant difference in pH between the pooled controls, 125 µg/L, or 1000 µg/L treatments ($p>0.05$). Alkalinity was also significantly different between treatments, (ANOVA $p<0.001$), with significantly higher values in the 250 µg/L, 500 µg/L, and 1000 µg/L treatments compared to the pooled controls (Tukey's HSD, $p<0.001$). There was no significant difference ($p>0.05$) in nutrient levels (PO_4, NH_3, NO_2, NO_3), temperature, or dissolved oxygen between treatments.

Table 5: Mean water quality (± SD) parameter at 96 h for avobenzone exposure.

Treatment	Temp (°C)	pH	DO (ppm)	Alk (ppm)	PO4 (ppm)	NH3 (ppm)	NO2 (ppm)	NO3 (ppm)
SW Control	26.28 (±0.41)	8.03 (±0.03)	7.88 (±0.05)	111.4 (±4.81)	0.24 (±0.07)	0.00 (±0.00)	0.01 (±0.00)	0.01 (±0.00)
MeOH Control	26.23 (±0.81)	7.98 (±0.05)	7.68 (±0.05)	112.70 (±1.62)	0.25 (±0.10)	0.00 (±0.00)	0.01 (±0.01)	0.01 (±0.00)
125 µg/L	25.68 (±0.28)	8.04 (±0.01)	7.83 (±0.45)	115.08 (±1.16)	0.21 (±0.06)	0.00 (±0.00)	0.02 (±0.01)	0.01 (±0.01)
250 µg/L	25.58 (±0.57)	8.09 (±0.03)	7.63 (±0.28)	119.24 (±0.49)	0.21 (±0.03)	0.00 (±0.00)	0.02 (±0.00)	0.02 (±0.01)
500 µg/L	25.75 (±0.30)	8.08 (±0.00)	7.75 (±0.17)	119.73 (±1.74)	0.24 (±0.04)	0.00 (±0.00)	0.01 (±0.00)	0.01 (±0.00)
1000 µg/L	25.70 (±0.55)	8.03 (±0.10)	7.83 (±0.22)	120.79 (±2.12)	0.27 (±0.07)	0.00 (±0.00)	0.02 (±0.01)	0.01 (±0.00)

Results for the analytical confirmation of exposure concentrations are pending so all threshold concentrations were estimated with nominal exposure concentrations.

Coral condition

Corals in the avobenzone exposure exhibited severe responses to high concentrations (Figure 3). Mean score proportions of coral conditions (±SE) at each time point are shown in Figure 4A. Corals in the seawater and methanol controls had no significant difference in condition throughout the exposure and only exhibited mild polyp retraction (retraction of tentacles and slight closure of the oral disk) at various time points beyond 8 h (Figure 3A – Figure 14D). Consistent polyp retraction was present in all treatments starting at different time points. The 500 µg/L and 1000 µg/L treatments exhibited polyp retraction at the first time point, 1 h into the exposure (Figure 3I and Figure 3K), corals in the 250 µg/L treatment had polyp retraction at 4 h and the 125 µg/L treatment had consistent polyp retraction starting at 8 h. Visible tissue attenuation was present beginning at 12 h in the 500 µg/L and 1000 µg/L treatments and 60 h in the 250 µg/L treatment. By 96 hours, there was moderate tissue attenuation in the 250 µg/L treatment (Figure 3H) and

severe tissue attenuation in the 500 µg/L and 1000 µg/L treatments (Figure 3J and Figure 3L). There was no visible bleaching, tissue swelling, or excessive mucous production throughout the exposure. Starting at 1 h into the exposure, a significant treatment effect was present (Kruskal-Wallis, $p<0.05$), with corals in the 1000 µg/L treatments scoring significantly higher than the pooled controls (Mann Whitney U Test, $p=0.01$). Corals in the 500 µg/L treatment had significant higher scores than the pooled controls starting at 4 h (Mann Whitney U Test, $p=0.001$). At 36 h, corals in the 125 µg/L and 250 µg/L treatments had significantly higher scores (Mann Whitney U Test, $p=0.04$) but only the 250 µg/L treatment had significantly higher scores at 60 h ($p=0.007$). After 72 h, corals in all treatments had significantly higher scores (Mann Whitney U Test, $p<0.05$). At 96 h, all treatments scored significantly higher than the pooled controls (Mann Whitney U Test, $p<0.01$) (Figure 4A).

Coral mortality

Mean percent mortality (±SE) at each time point are shown in Figure 4B. Significant treatment effects were observed starting at 24 h (Kruskal-Wallis, $p<0.001$). Post-hoc analysis confirmed significantly higher mortality percentages in the 500 µg/L and 1000 µg/L treatments (Mann Whitney U Test, $p=0.001$). At 84 h, the 250 µg/L treatments also had significantly higher mortality (Mann Whitney U Test, $p=0.009$). At 96 hours several fragments in the 1000 µg/L treatment had 100% mortality (Figure 3L). Corals in the 500 µg/L treatment had as high as 85% mortality (Figure 3J) and the 250 µg/L treatment only had up to 5% mortality (Figure 3H). At the 8 d post-exposure time point the 500 µg/L and 1000 µg/L treatments still showed significantly higher mortality than the pooled controls (Mann Whitney U Test, $p=0.001$). Some tissue recovery was seen in corals with attenuation (Figure 5B and Figure 5D).

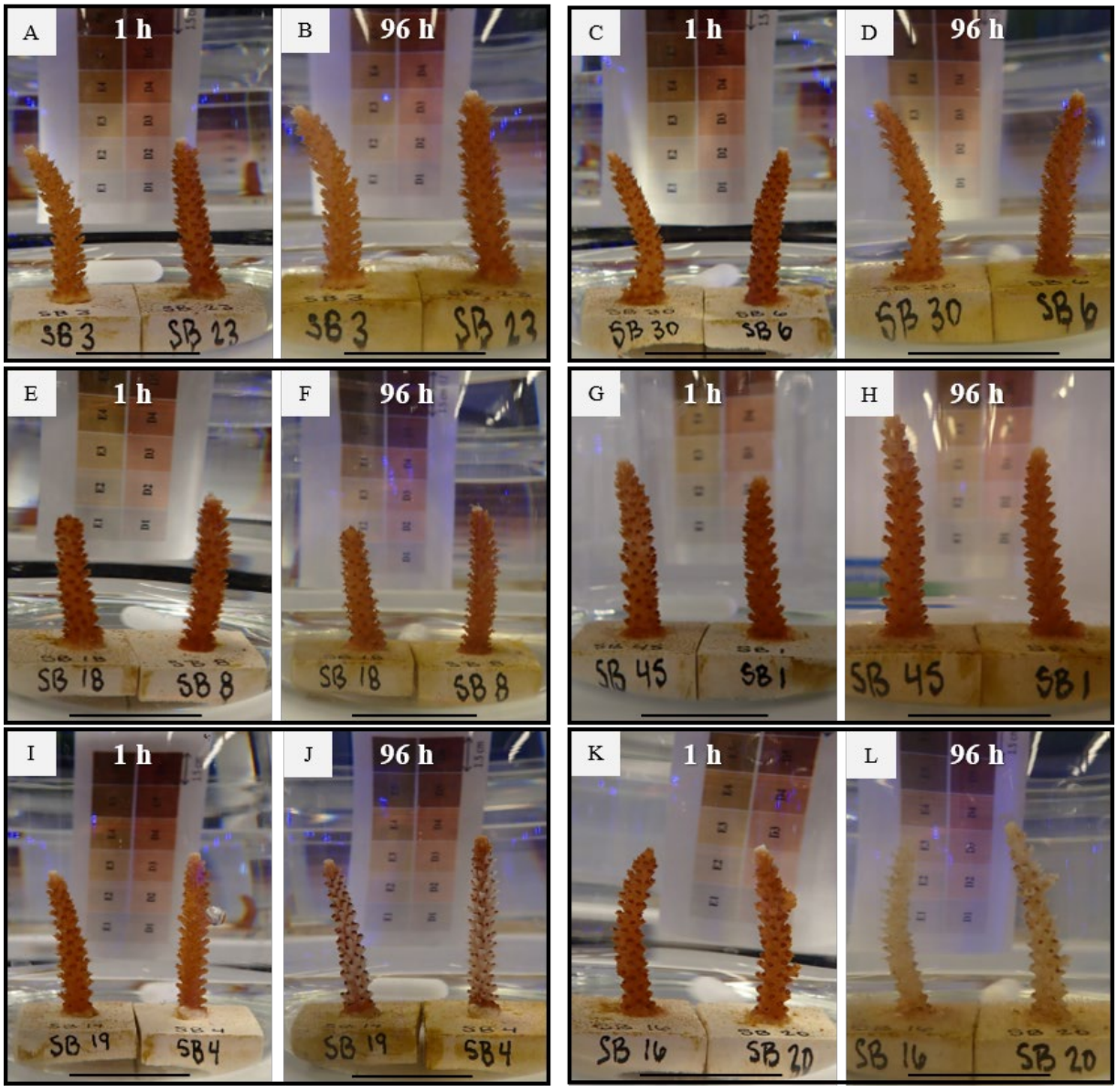

Figure 3. *Acropora cervicornis*. Physical coral response at the start (1 h) and end (96 h) of the avobenzone exposure for each exposure concentration. Seawater control at (**A**) 1 h and (**B**) 96 h, methanol control at (**C**) 1 h and (**D**) 96 h, 125 µg/L at (**E**) 1 h and (**F**) 96 h, 250 µg/L at (**G**) 1 h and (**H**) 96 h, 500 µg/L at (**I**) 1 h and (**J**) 96 h, 1000 µg/L at (**K**) 1 h and (**L**) 96 h. Corals appear healthy in the seawater and methanol controls and the 125 µg/L treatment with consistent color and extended polyps. Corals in the 250 µg/L treatment at 96 h showed polyp retraction and a small degree of tissue attenuation around the corallites. Corals in the 250 µg/L treatment showed severe tissue attenuation and retracted polyps. Total mortality was observed in the 1000 µg/L treatment. Scale bars are 2.5 cm.

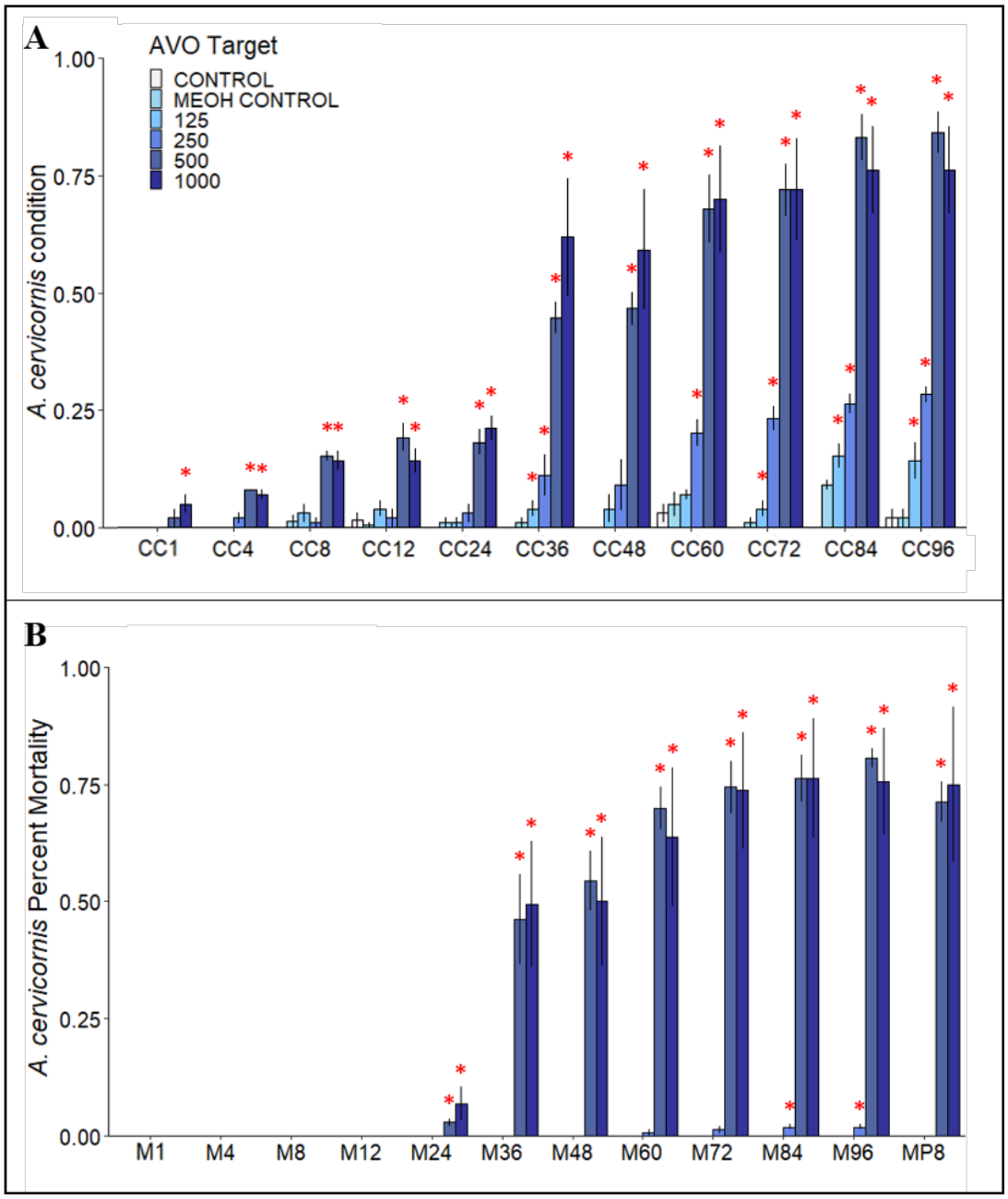

Figure 4. (**A**) Mean coral condition score proportion (±SE) throughout the 96 h avobenzone exposure based on diagnostic criteria in Table 2. (**B**) The mean percent mortality of each treatment at each time point during the exposure and 8 d post-exposure, expressed as percent mortality (±SE). Red stars (*) denote significant differences ($p < 0.05$) from the pooled seawater and methanol controls (40 µl/L MeOH).

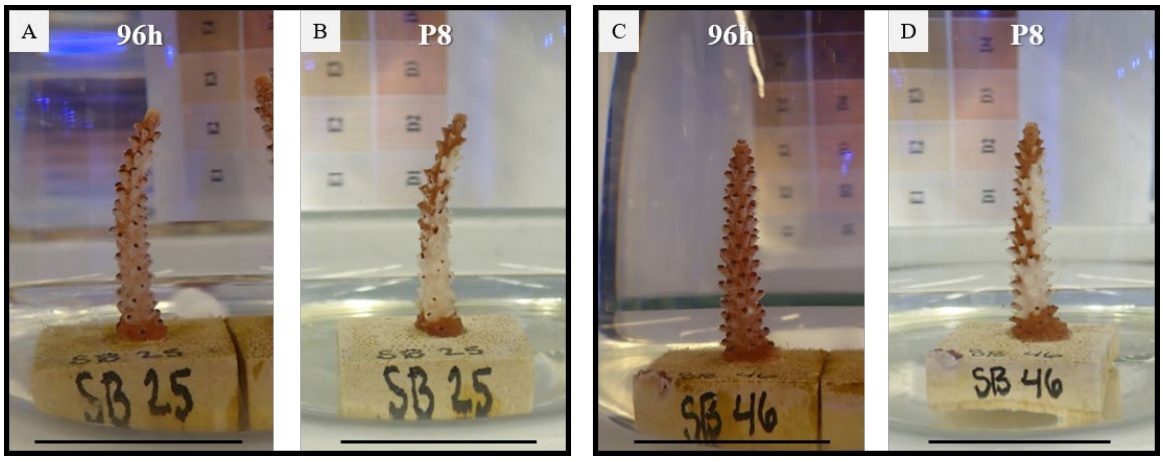

Figure 5. *Acropora cervicornis*. Physical coral response at the end (96 h) of the avobenzone exposure and 8 d post-exposure (P8). Coral from the 500 µg/L treatment at (**A**) 96 h and (**B**) 8 d. Coral from the 1000 µg/L treatment at (**C**) 96 h and (**D**) 8 d. In the 8 d post-exposure the already attenuated tissues were fully lost from the coral while the remaining tissue appeared to start healing. Scale bars are 2.5 cm.

Photosynthetic efficiency

Mean photosynthetic efficiency measurements (±SE) are shown in Figure 6A. Two fragments in the 1000 µg/L treatment that reach 100% mortality were not included in these data due low fluorescence readings. There was no significant difference in yield between the pooled controls and treatments at any time (Kruskal-Wallis, $p>0.05$).

Calcification

Mean skeletal growth rates (mg/d) (±SE) for each treatment at the end of the 96 h exposure and at 8 d post-exposure are shown in Figure 6B. Significant treatment effects were observed after the exposure (ANOVA, $p<0.001$). Post-hoc analysis of treatment effects showed significantly lower growth rates in all treatments (125 µg/L, 250 µg/L, 500 µg/L, and 1000 µg/L) compared to the pooled controls (Dunnett, $p<0.05$). Growth rate remained significantly different between treatments 8 d post-exposure (ANOVA, $p=0.001$) with the 250 µg/L, 500 µg/L, and 1000 µg/L treatments showing significantly lower growth rates (Dunnett, $p=0.02$, $p=0.007$, and $p=0.002$ respectively).

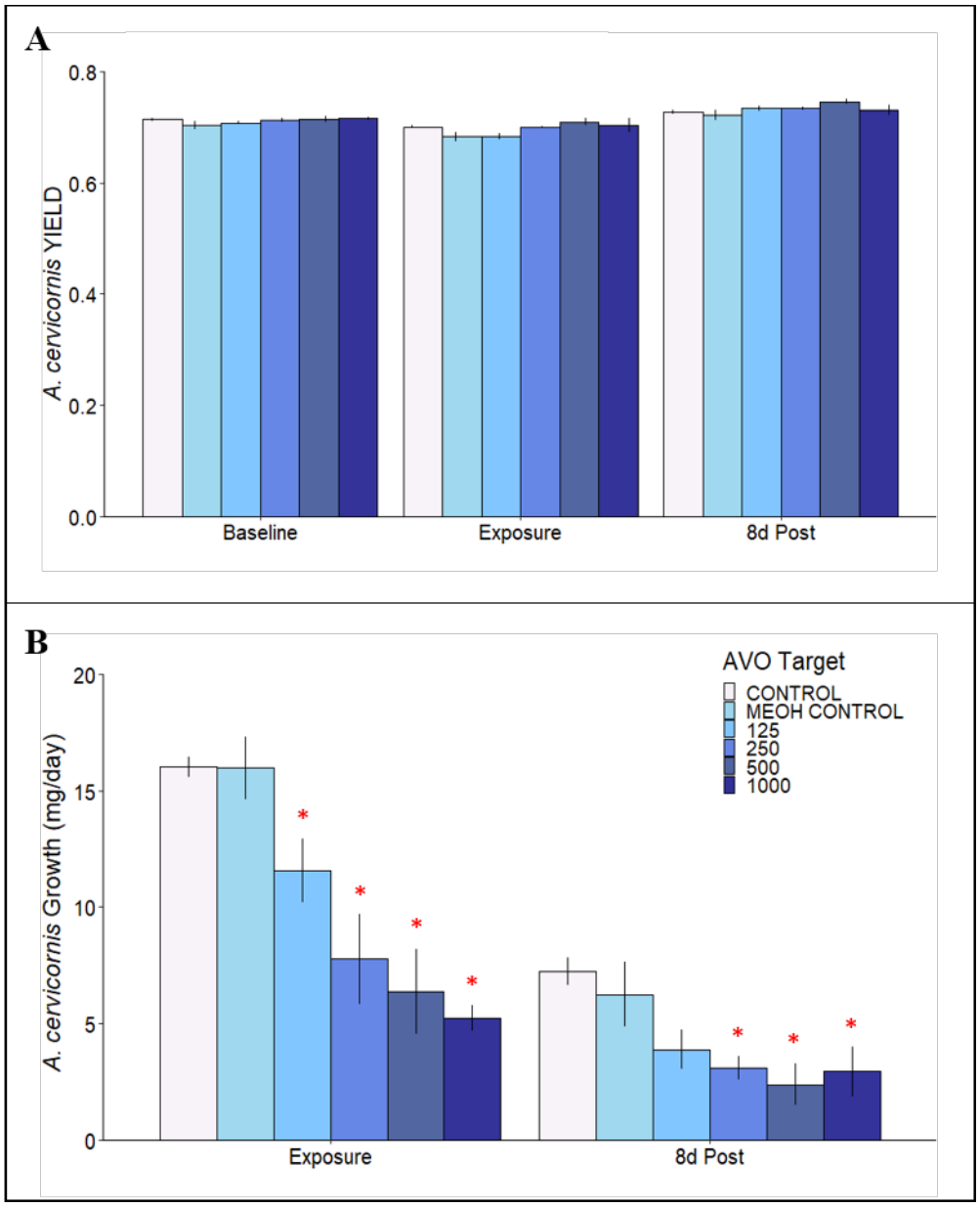

Figure 6. (**A**) Mean dark-adapted maximum quantum yield (±SE) for each treatment before the exposure (baseline), after the 96 h exposure (exposure), and 8 d post-exposure (8 d Post). (**B**) Mean growth rate of each treatment during each time period, expressed as growth (mg/day) (±SE). Red stars (*) denote significant differences ($p < 0.05$) from the pooled seawater and methanol controls (40 µl/L MeOH).

Cellular and tissue changes

Exposure to avobenzone negatively impacted cellular and tissue health in *A. cervicornis*. Coral fragments were fixed immediately following the 96 h exposure and were scored based on epidermal mucocytes (EM), costal tissue loss (CTL), zooxanthellae in the surface body wall (ZSBW), cnidoglandular band epidermal mucocytes (CBEM), cnidoglandular band degeneration (CB), cell dissociation of mesenterial filaments (MF), gastrodermal architecture (GA), and calicodermis (C). Average score proportions for each treatment are shown in Figure 7. Total histological score proportions (Figure 7A) were calculated from the sum of the scores for each cellular component observed (Figure 7B). Significant treatment effects were observed in total histological score proportions (ANOVA, $p<0.001$). Post hoc analysis revealed significantly higher scores in the three highest treatments, 250 µg/L, 500 µg/L, and 1000 µg/L (Dunnett, $p=0.01$, $p=0.0001$, $p=0.0002$, respectively).

Significant treatment effects were observed in EM (ANOVA, $p = 0.03$), with significant effects observed in the 250 µg/L, 500 µg/L, and 1000 µg/L treatments (Dunnett, $p<0.01$). Mucocytes in the controls were in fair condition with some irregularity in size and pale to dark staining mucus along with visible ciliated support cells (Figure 8A). In the low treatments, 125 µg/L and 250 µg/L, there was a higher presence of hypertrophied and ruptured mucocytes, with the loss of some support cells (Figure 7C). Although, the lowest treatment was not significantly worse than the pooled controls. The corals in the 500 µg/L and 1000 µg/L treatments showed a marked to severe condition with atrophying of the epidermis, loss of mucocytes and full ablation of the epidermis in some instances (Figure 8E and Figure 8G). A significant treatment effect was also present for CTL (Kruskal Wallis, $p<0.001$); all treatments were significantly more effected than the pooled controls (Mann Whitney U Test, $p<0.01$). Control corals showed minimal change, with thinning of the epidermis over costae and very minimal costae exposed (Figure 8B). With increasing treatment levels, there was a higher amount of tissue loss and exposed skeleton with most to all of the costae being exposed in the highest treatments (Figure 8D, Figure 8F, and Figure 8H). No significant effects were seen in zooxanthellae in the surface body wall (ANOVA, $p>0.05$). Zooxanthellae appeared mostly healthy with some presence of mishappen cells and atrophy.

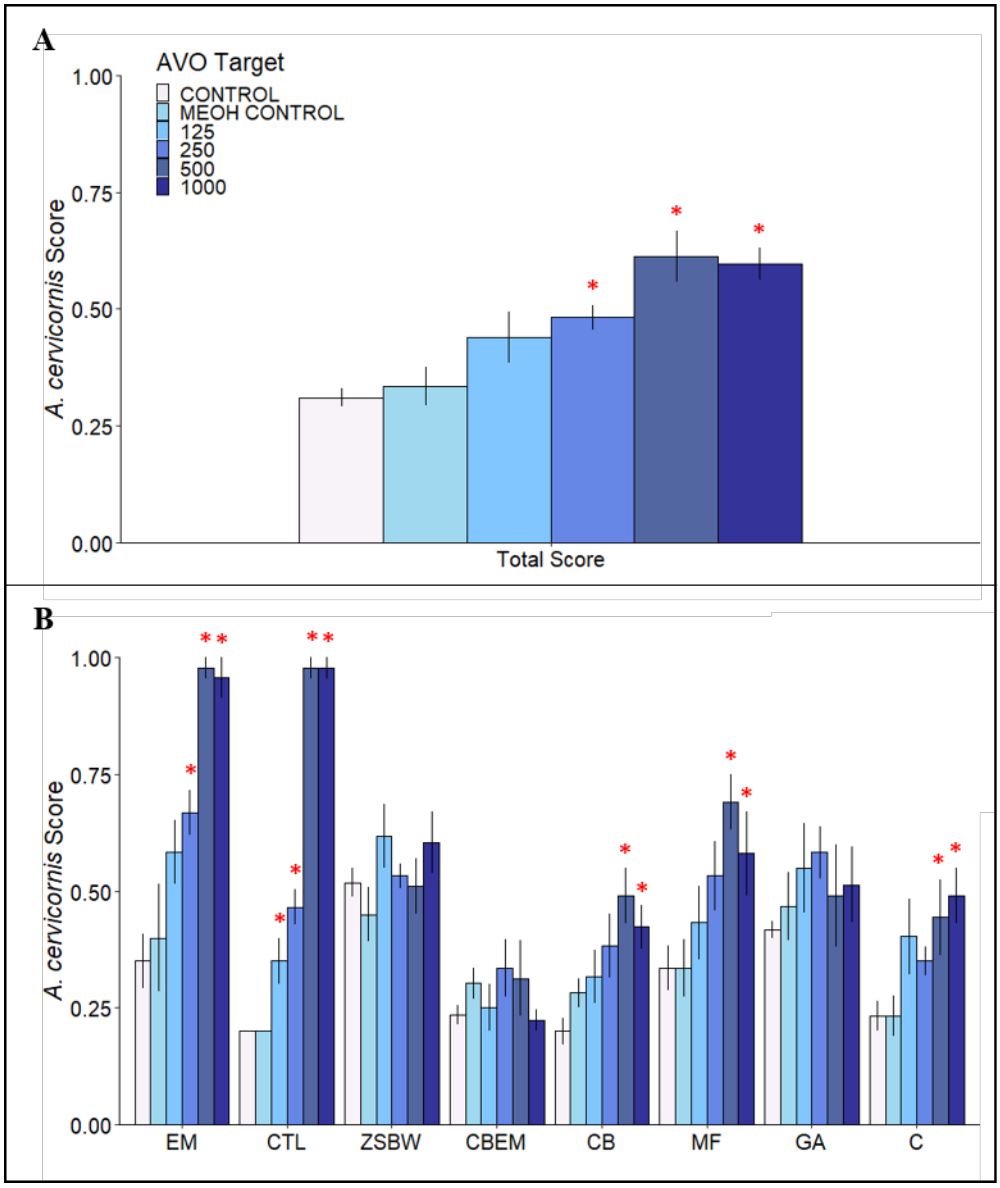

Figure 7. Mean histological score proportions (±SE) for each treatment after the 96 h avobenzone exposure. (**A**) Total mean histological scores are the proportions of the summed individual cell type scores. (**B**) Mean score proportions for each of the cell types observed; epidermal mucocytes (EM), costal tissue loss (CTL), zooxanthellae in the surface body wall (ZSBW), cnidoglandular band epidermal mucocytes (CBEM), cnidoglandular band degeneration (CB), cell dissociation on mesenterial filaments (MF), gastrodermal architecture (GA), and calicodermis (C). Red stars (*) denote significant differences ($p < 0.05$) from the pooled seawater and methanol controls (40 µl/L MeOH).

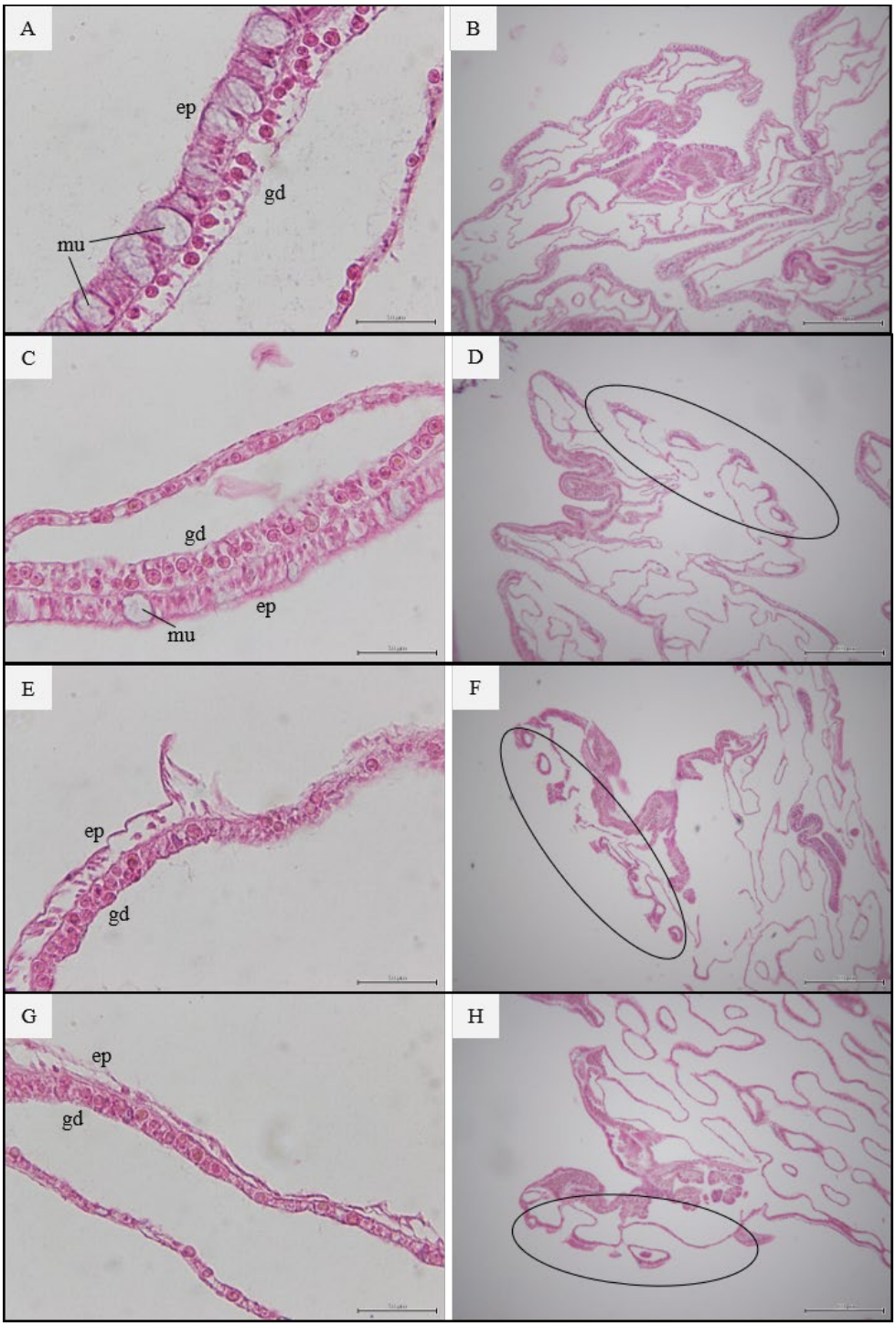

Figure 8. Histological sections of *Acropora cervicornis* surface body wall and polyps after the avobenzone exposure for the seawater control and the highest three treatments. (**A**) The surface body wall and (**B**) polyp in the seawater control. (**C**) The surface body wall and (**D**) polyp in the 250 µg/L treatment. (**E**) The surface body wall and (**F**) polyp in the 500 µg/L treatment. (**G**) The surface body wall and (**H**) polyp in the 1000 µg/L treatment. Ellipses surround areas of costal tissue loss. Scale bar = 50 µm for A, C, E, and G and 500 µm for B, D, F, and H. ep= epidermis, gd= gastrodermis, mu= mucocytes.

There were no significant effects seen in CBEM ($p>0.05$). Throughout all treatments, cnidoglandular bands appeared to be less than 50% composed of mucocytes, with only a few fragments showing an increased presence. However, there were significant treatment effects in CB (ANOVA, $p=0.01$) with a significant necrosis in the 500 µg/L and 1000 µg/L treatments (Dunnett, $p=0.006$, $p=0.049$, respectively). Controls showed normal to minimal architecture with the presence of nematocytes, granular gland cells, columnar cells and a clear terminal bar (Figure 9A and B). High treatments exhibited reductions in nematocytes and granular gland cells, breaks in the terminal bar, and necrosis (Figure 9C and Figure 9D). Also, there were significant treatment effects seen in MF (ANOVA, $p=0.006$) with significant necrosis and vacuolation in the 500 µg/L and 1000 µg/L treatments (Dunnett, $p=0.003$, $p=0.04$, respectively). The high treatments were characterized as moderate to marked with an increased presence of mucocytes, vacuolation, gaps in the terminal bar, and cell loss (Figure 9C and Figure 9D).

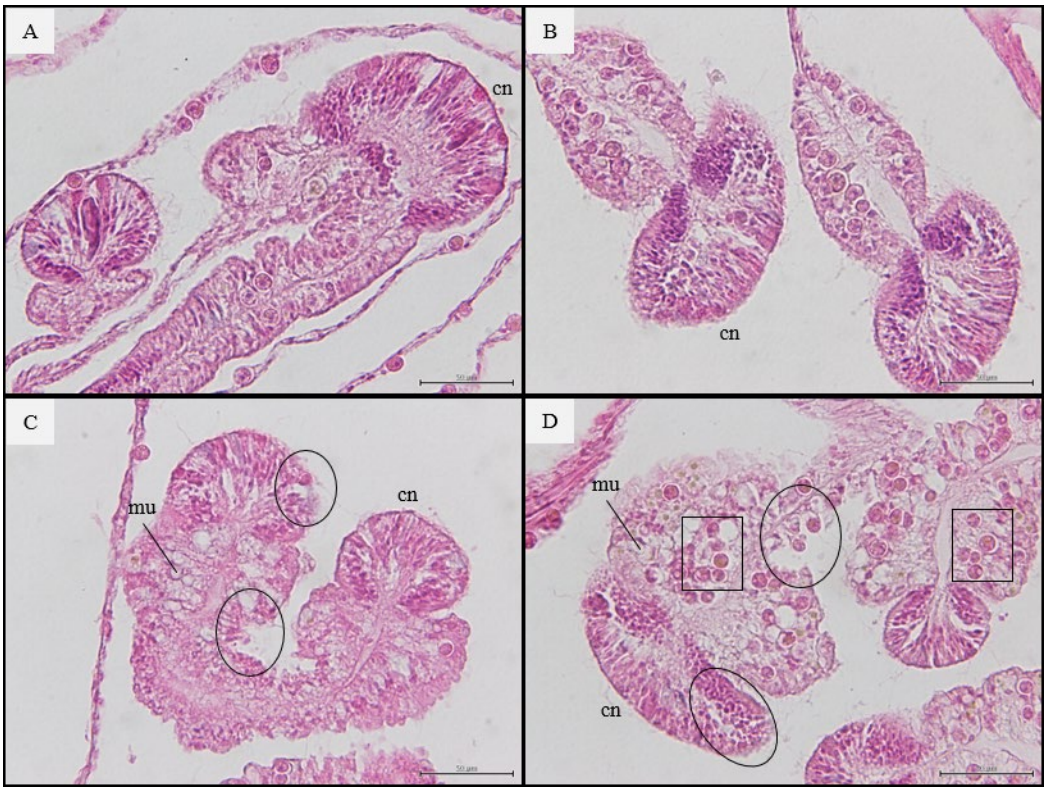

Figure 9. Histological sections of *Acropora cervicornis* cnidoglandular bands and mesenteries after the avobenzone exposure for the seawater and methanol controls and the highest two treatments. (**A**) Seawater control (**B**) methanol control (**C**) 500 µg/L treatment, and (**D**) 1000 µg/L treatment. Ellipses surround areas of necrotic cells. Boxes surround areas of vacuolation. Scale bar = 50 µm. cn= cnidoglandular band, mu= mucocytes.

A significant treatment effect was seen in C (ANOVA, p=0.01) with a significant reduction in calicoblasts in the 500 µg/L and 1000 µg/L treatments (Dunnett, p=0.03, p=0.008, respectively) (Figure 10B). In regard to GA, there was some swelling present and increased lipid droplets in some fragments however there were no significant treatment effects (ANOVA, p>0.05).

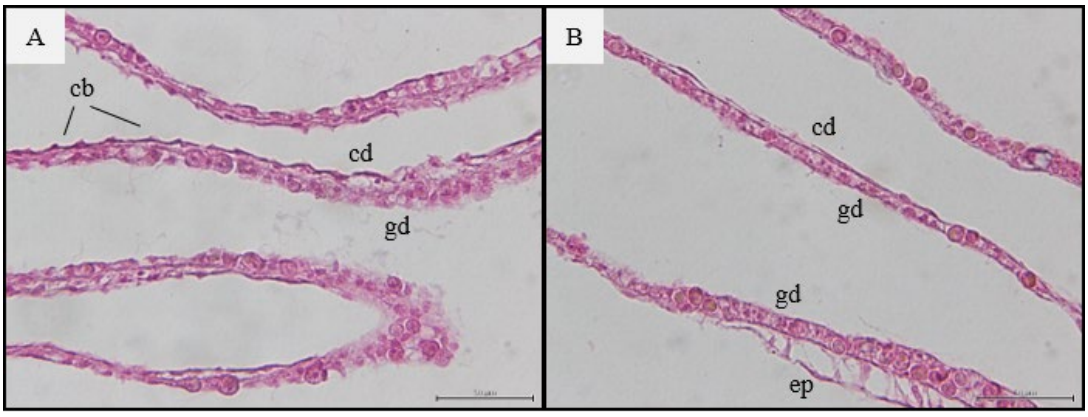

Figure 10. Histological sections of *Acropora cervicornis* calicodermis. (**A**) Seawater control (**B**) methanol control (**C**) 500 µg/L treatment, and (**D**) 1000 µg/L treatment. Scale bar = 50 µm. ep= epidermis, gd= gastrodermis, cd= calicodermis, cb= calicoblasts.

Toxicity thresholds

A summary of all toxicity thresholds following the 96 h exposure to avobenzone is detailed in Table 6.

Table 6: Effect concentrations (µg/L) after 96 h avobenzone exposure. ns=not significant.

Coral Health	NOEC	LOEC	50% Effect Concentrations	95% Confidence Interval
Coral Condition	0	125	EC50: 324.5	261.0 - 388.0
Photosynthetic Efficiency	1000	ns	ns	ns
Growth	0	125	IC50: 148.2	70.0 – 226.4
Cellular and Tissue Health	125	250	EC50: 1406.3	9.4 - 2803.2
Epidermal Mucocytes	125	250	EC50: 216.4	122.6 - 310.3
Costal Tissue Loss	0	125	EC50: 294.5	262.1 – 326.9
Cnidoglandular Band	250	500	ns	ns
Mesenterial Filaments	250	500	ns	ns
Calicodermis	250	500	ns	ns
Mortality	125	250	LC50: 407.6	330.8 – 484.4

All sublethal (coral condition) and lethal (mortality) thresholds were estimated using dose response curves with significant model fits ($p<0.05$) from each 24 h interval throughout the 96 h exposure (Figure 11). The 24 h EC50 was 2991.3 µg/L (95% CI: 1326.5 - 4656.1) (Figure 11A). The 48 h EC50 lowered to 653.4 µg/L (95% CI: 478.0 - 828.9) (Figure 11B). The 72 h EC50 was 384.9 µg/L (95% CI: 301.7 - 468.0) and the 72 h LC50 was 420.3 µg/L (95% CI: 356.1 - 484.5) (Figure 11C and Figure 13E). The 96 h EC50 was 324.5 µg/L (95% CI: 261.0 - 388.0) and the 96 h LC50 was 407.6 µg/L (95% CI: 330.8 – 484.4) (Figure 11D and Figure 13F).

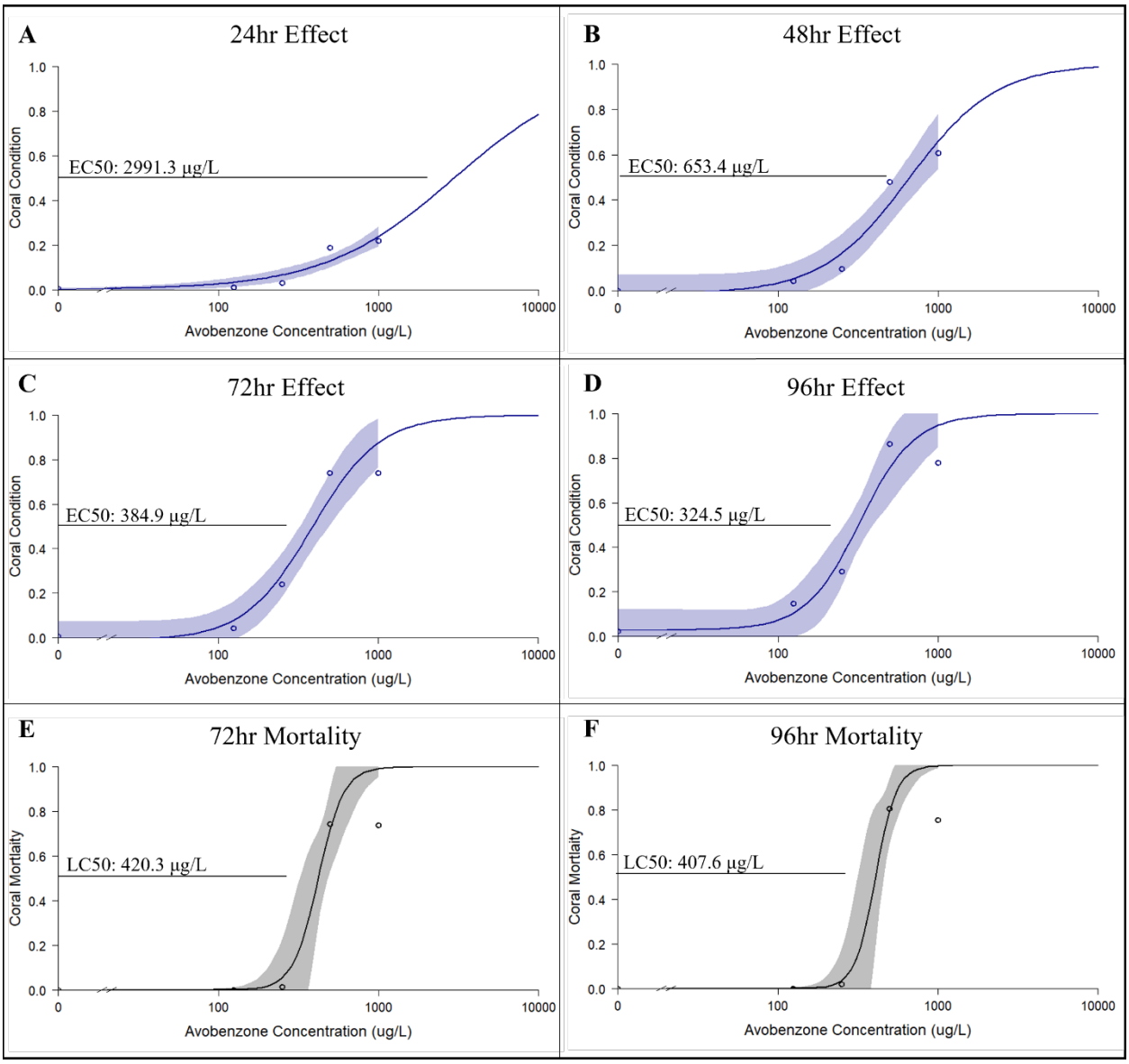

Figure 11. Avobenzone dose-response curves based on coral condition scores (EC50) and percent mortality (LC50) when significant model fits were present throughout the 96 h exposure. EC50s at (**A**) 24 h, (**B**) 48 h, (**C**) 72 h, and (**D**) 96 h. LC50s at (**E**) 72 h and (**F**) 96 h.

Sublethal inhibition thresholds (IC50) were estimated for dark-adapted maximum quantum yield and coral calcification rates (Figure 12). As there were no significant effects on Fv/Fm after the 96 h exposure, there was no significant model fit and no threshold was estimated (Figure 12A). The observed effects on coral calcification allowed a significant model fit when treatment growth rates were modeled as percent of the average control growth rate (p=0.002). The 96 h IC50 was 319.0 µg/L (95% CI: 128.8 - 509.2) (Figure 12B).

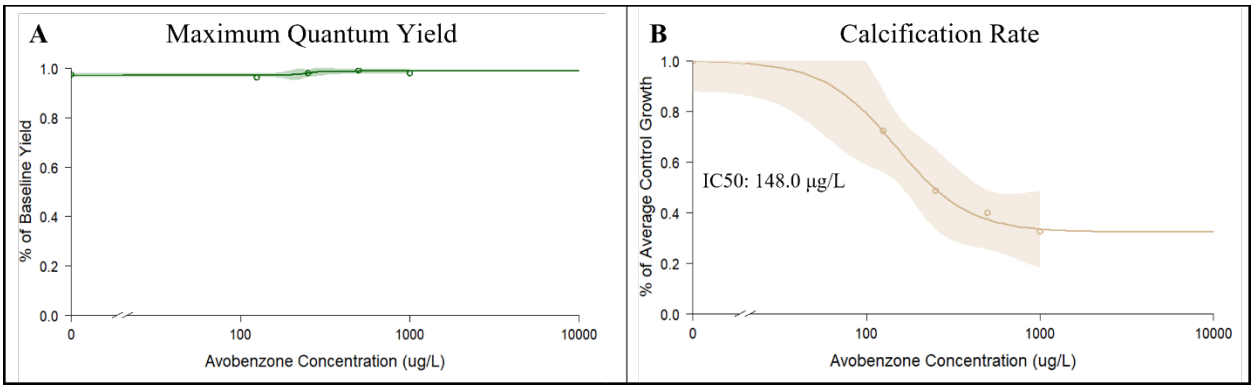

Figure 13. Avobenzone dose-response curves for effects on (**A**) dark-adapted maximum quantum yield at 96 h and (**B**) coral calcification rates (plotted as percent of average control growth rates) at 96 h.

Sublethal effect thresholds were also estimated for significant histological parameters. Model fits were significant ($p<0.05$) for total histological score proportions, EM score proportions, and CTL score proportions (Figure 13). All other histological parameters either did not show significant effects or did not produce significant dose response curves. Total histological score proportions 96 h EC50 was 1406.3 µg/L (95% CI: 9.4 - 2803.2) (Figure 13A). EM score

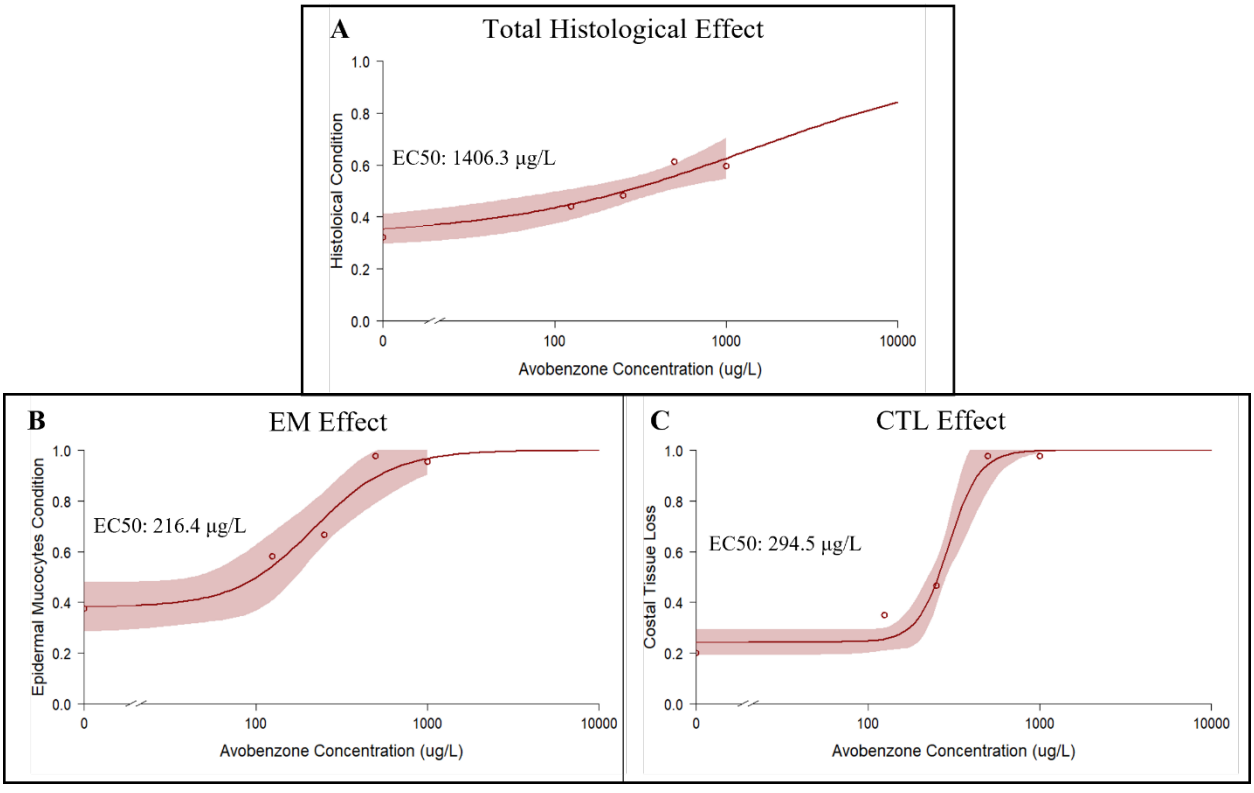

Figure 12. Avobenzone dose-response curves for (**A**) effects total histological score, (**B**) epidermal mucocyte condition, and (**C**) costal tissue loss at the endpoint of the 96 h exposure.

proportions had a 96 h EC50 of 216.4 µg/L (95% CI: 122.6 - 310.3) (Figure 13B). Lastly, CTL score proportions had a 96 h EC50 of 294.5 µg/L (95% CI: 262.1 – 326.9) (Figure 13C).

RESULTS FROM EXPERIMENT 2 (HOMOSALATE)

Water quality

Mean water quality parameters at the end of the 96 h exposure are summarized in Table 7. There were significantly different pH values between treatments (ANOVA, $p<0.001$). Post-hoc analysis showed significantly higher values in the 1800 µg/L and 5400 µg/L treatments (Tukey's HSD, $p<0.01$). Dissolved oxygen had significantly different values between treatments (ANOVA, $p<0.001$). Significantly lower values were seen in the 1800 µg/L, and 5400 µg/L treatments (Tukey's HSD, $p<0.001$). Alkalinity had significantly different values between treatments (Kruskal-Wallis, $p=0.009$) with significantly higher values in the 1800 µg/L and 5400 µg/L treatments (Multiple comparisons, $p=0.009$ and $p=0.002$, respectively). There was no significant difference ($p>0.05$) in temperature or nutrient levels (PO_4, NH_3, NO_2, NO_3) between treatments.

Table 7: Mean water quality (± SD) parameter at 96 h for homosalate exposure.

Treatment	Temp (°C)	pH	DO (ppm)	Alk (ppm)	PO4 (ppm)	NH3 (ppm)	NO2 (ppm)	NO3 (ppm)
SW Control	24.85 (±0.19)	8.14 (±0.02)	8.07 (±0.10)	105.23 (±3.21)	0.11 (±0.06)	0.00 (±0.00)	0.02 (±0.01)	0.02 (±0.01)
MeOH Control	24.60 (±0.12)	8.14 (±0.02)	8.08 (±0.03)	108.09 (±2.86)	0.09 (±0.03)	0.00 (±0.00)	0.01 (±0.00)	0.02 (±0.01)
200 µg/L	24.73 (±0.13)	8.16 (±0.01)	8.05 (±0.05)	110.30 (±3.67)	0.09 (±0.01)	0.00 (±0.00)	0.02 (±0.00)	0.01 (±0.00)
600 µg/L	24.65 (±0.06)	8.17 (±0.01)	7.98 (±0.02)	110.70 (±0.39)	0.11 (±0.03)	0.00 (±0.00)	0.02 (±0.00)	0.01 (±0.00)
1800 µg/L	24.75 (±0.06)	8.18 (±0.02)	7.87 (±0.08)	112.89 (±1.84)	0.08 (±0.01)	0.00 (±0.00)	0.02 (±0.00)	0.01 (±0.01)
5400 µg/L	24.68 (±0.10)	8.19 (±0.02)	7.85 (±0.02)	113.21 (±1.46)	0.08 (±0.02)	0.00 (±0.00)	0.02 (±0.00)	0.01 (±0.00)

Results for the analytical confirmation of exposure concentrations are pending so all threshold concentrations were estimated with nominal exposure concentrations.

Coral condition

Corals in the homosalate exposure exhibited moderate responses to high concentrations (Figure 14). Mean score proportions of coral condition at each time point are shown in Figure 15A. Corals in the seawater and seawater/methanol controls had no significant difference in condition over the exposure and only exhibited mild polyp retraction at inconsistent time points beyond 8 h (Figure 14A – Figure 14D). At the start of the exposure (1 h), polyp retraction was present in all homosalate treatments (Figure 14E, Figure 14G, Figure 14I, and Figure 14K). These observations stayed consistent until 24 h when some of the polyps became slightly more extended in the 200 µg/L and 600 µg/L treatments. Starting at 36 hours, polyp retraction remained consistent in the 600 µg/L, 1800 µg/L and 5400 µg/L treatments for the remainder of the 96 h exposure (Figure 14H, Figure 14J, and Figure 14L). Tissue attenuation was present in the 5400 µg/L treatment at 24 h. After 48 h, small amounts of tissue attenuation were observed in corals in the 600 µg/L treatment. By 72 h, several fragments in each of the top three treatments, 600 µg/L, 1800 µg/L, and 5400 µg/L, showed signs of tissue attenuation. At the end of the 96 h exposure there was minimal tissue attenuation in the 600 µg/L (Figure 14H) and moderate tissue attenuation in the 1800 µg/L, and 5400 µg/L treatments (Figure 14J and Figure 14L). There was no visible bleaching, tissue swelling, or excessive mucus production throughout the exposure. Starting at 1 h, corals in the 200 µg/L, 600 µg/L, 1800 µg/L and 5400 µg/L treatments scored significantly higher than the pooled controls (Mann Whitney U Test, $p<0.01$). At 24 h only the 1800 µg/L and 5400 µg/L treatments had significantly higher scores than the pooled controls (Mann Whitney U Test, $p<0.01$); however, at 36 h, all treatments were again significantly higher (Mann Whitney U Test, $p<0.05$). After 48 h there was no longer a significant effect in the 200 µg/L treatment (Mann Whitney U Test, $p>0.05$), except at 84 h ($p=0.02$). At the end of the 96 h exposure, the 600 µg/L, 1800 µg/L and 5400 µg/L treatments scored significantly higher than the pooled controls (Mann Whitney U Test, $p<0.01$) (Figure 15A).

Coral mortality

Mean mortality percentages at each time point are shown in Figure 15B. Significant treatment effects (Kruskal-Wallis, $p<0.05$) were observed starting at 60 h in the 5400 µg/L treatment (Mann Whitney U Test, $p=0.01$). Only the 5400 µg/L treatment, with as high as 20% mortality, had significantly higher percent mortality compared to the pooled controls at 96 h (Mann Whitney U Test, $p=0.01$). There were no significant treatment effects at the 7 d post-exposure time point (Kruskal-Wallis, $p>0.05$). Minimal tissue recovery was seen in corals 7 d post-exposure (Figure 16).

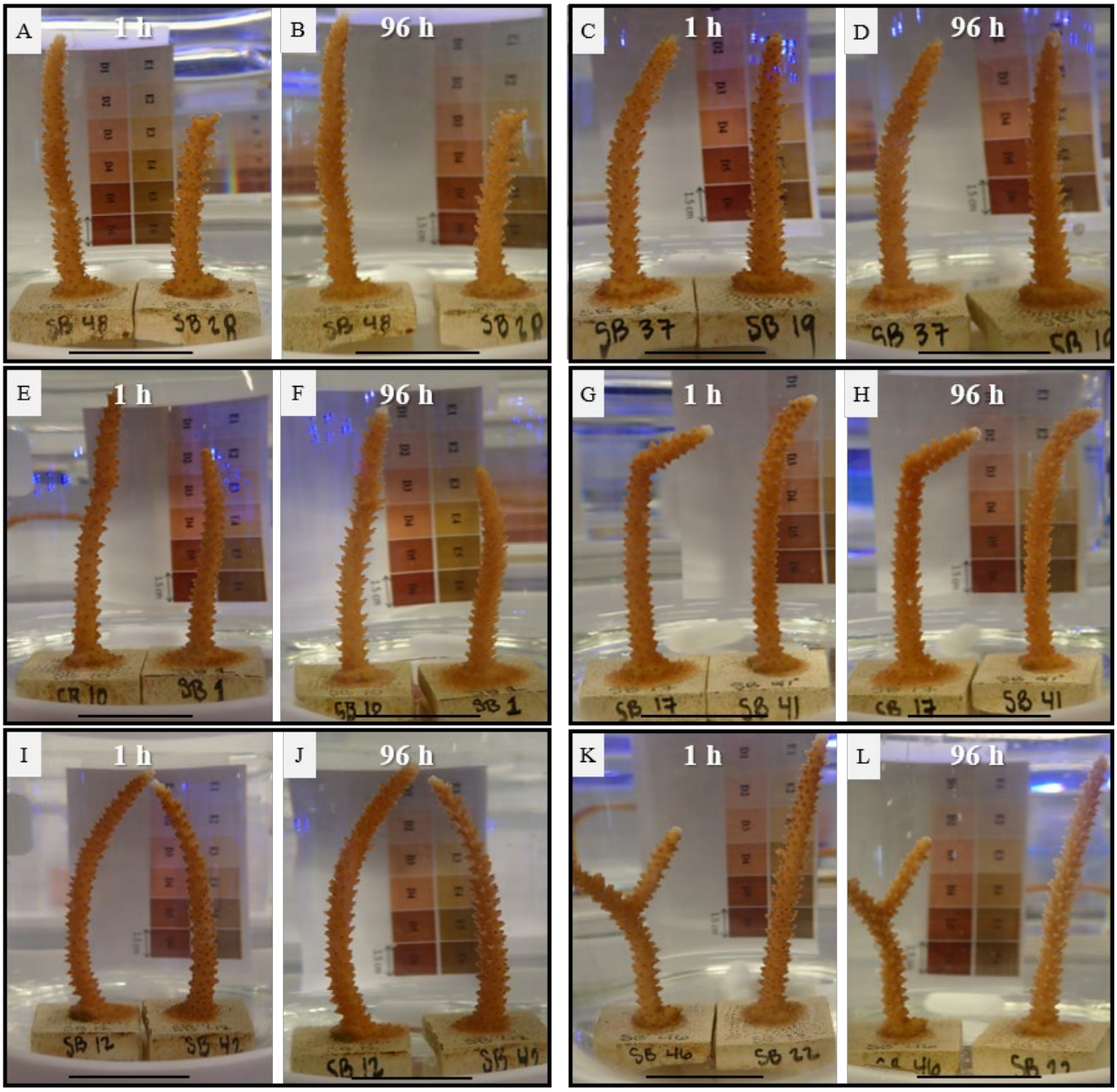

Figure 14. *Acropora cervicornis*. Physical coral response at the start (1 h) and end (96 h) of the avobenzone exposure for each exposure concentration. Seawater control at (**A**) 1 h and (**B**) 96 h, methanol control at (**C**) 1 h and (**D**) 96 h, 200 µg/L at (**E**) 1 h and (**F**) 96 h, 600 µg/L at (**G**) 1 h and (**H**) 96 h, 1800 µg/L at (**I**) 1 h and (**J**) 96 h, 5400 µg/L at (**K**) 1 h and (**L**) 96 h. Corals appear healthy in the seawater and methanol controls with consistent color and extended polyps. Corals in the 1800 µg/L and 5400 µg/L treatments at 96 h showed polyp retraction and a small degree of tissue attenuation around the corallites. Scale bars are 2.5 cm.

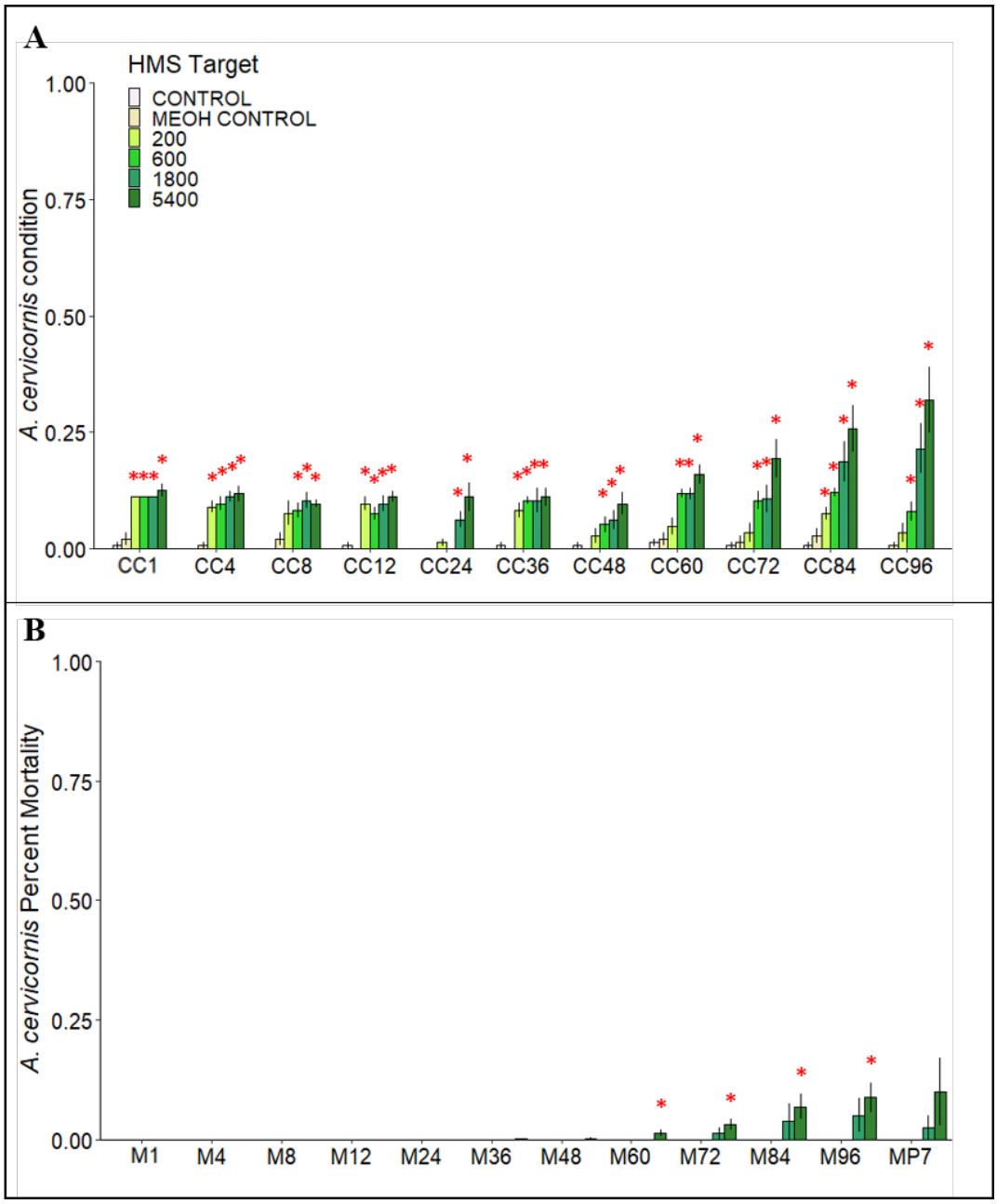

Figure 15. (**A**) Mean coral condition score proportion (±SE) throughout the 96 h homosalate exposure based on diagnostic criteria from Table 2. (**B**) The mean percent mortality of each treatment at each time point during the exposure and 7 d post-exposure, expressed as percent mortality (±SE). Red stars (*) denote significant differences ($p < 0.05$) from the pooled seawater and methanol controls (100 µl/L MeOH).

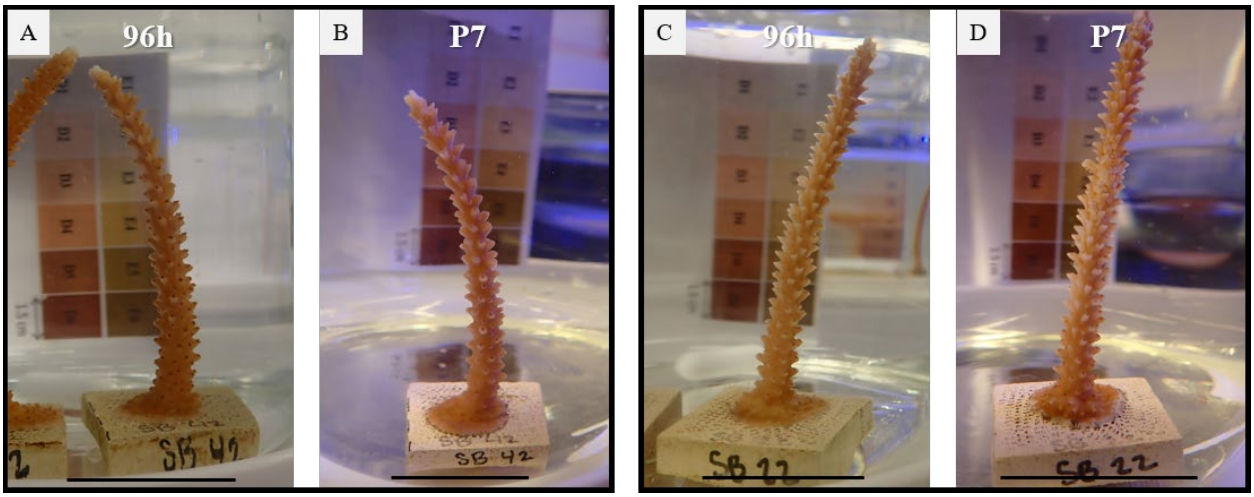

Figure 16. *Acropora cervicornis*. Physical coral response at the end (96 h) of the avobenzone exposure and 8 d post-exposure (P7). Coral from the 1800 µg/L treatment at (**A**) 96 h and (**B**) 7 d. Coral from the 5400 µg/L treatment at (**C**) 96 h and (**D**) 7 d. At 7 d post-exposure the *A. cervicornis* fragment in the 1800 µg/L treatment does not appear to regrow any tissue around the corallites, and the polyps are more severely retracted. At 7 d post-exposure, in the 5400 µg/L treatment, the coral fragment seems to have more tissue attenuation in the middle of the fragment. Scale bars are 2.5 cm.

Photosynthetic efficiency

Mean dark-adapted maximum quantum yields (Fv/Fm) are shown in Figure 17A. There was no significant difference in yield between the pooled controls and treatments at 96 h or after 7 d of recovery (ANOVA, $p>0.05$).

Calcification

Mean normalized skeletal growth rates, expressed as a percent of the baseline daily growth rate, for each treatment after the 96 h exposure and 7 d post-exposure are shown in Figure 17B. There was no significant difference in the baseline growth rates (Kruskal Wallis, $p>0.05$). At the end of the 96 h exposure, negative growth values were recorded for some fragments in all treatments, including both controls. High variability was seen in exposure growth rates and no significant treatment effects were observed (Kruskal Wallis $p>0.05$). Growth rates at 7 d post-exposure had significant effects ($p=0.01$). Post-hoc analysis showed the 600 µg/L, 1800 µg/L and 5400 µg/L treatments had significantly lower growth rates than the pooled controls (Mann Whitney U Test, $p<0.05$).

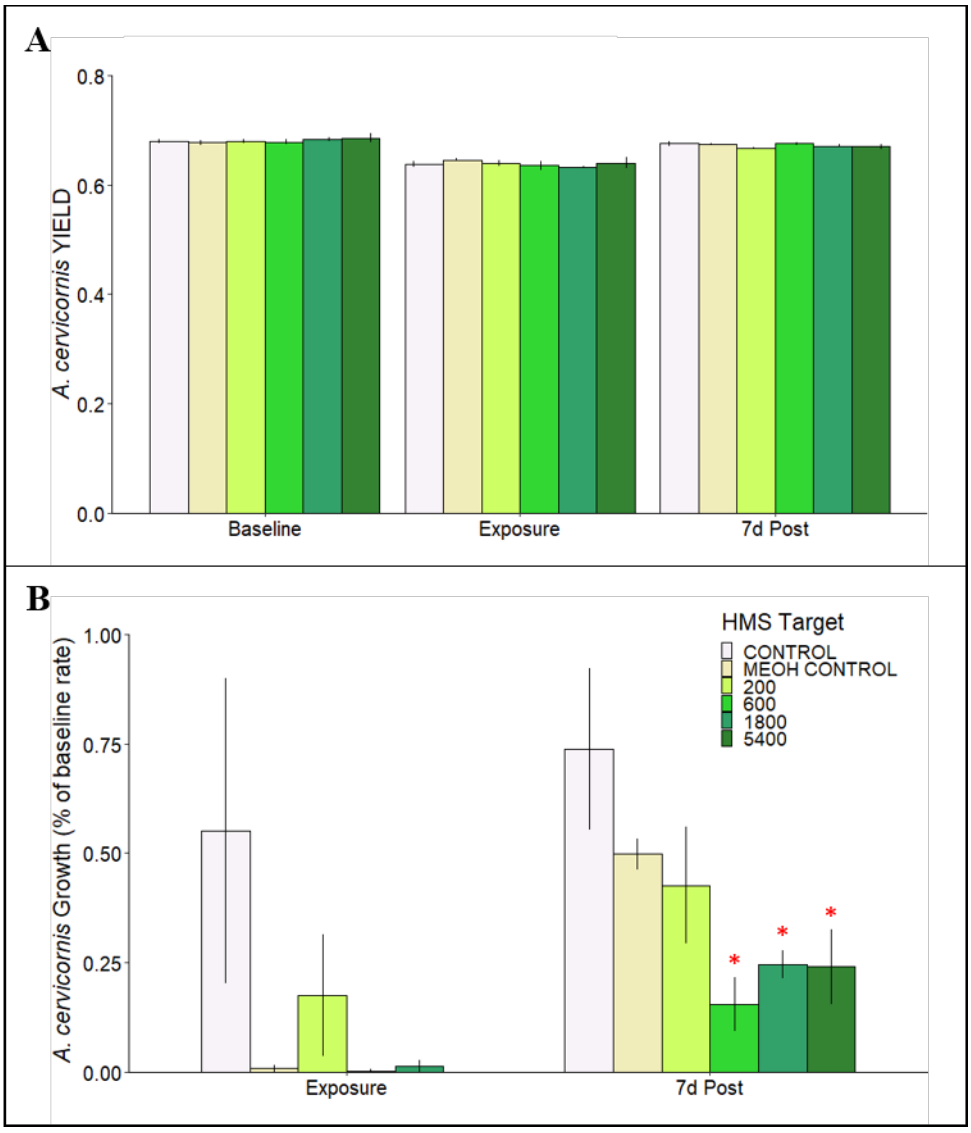

Figure 17. (**A**) Mean dark-adapted maximum quantum yield (±SE) for each treatment before the exposure (baseline), after the 96 h exposure (exposure), and 7 d post-exposure (7 d Post). (**B**) Mean normalized growth rate of each treatment during each time period, expressed as percent of the baseline growth rate. Red stars (*) denote significant differences ($p < 0.05$) from the pooled seawater and methanol controls (100 µl/L MeOH).

Cellular and tissue changes

Exposure of homosalate to *A. cervicornis* negatively impacted cellular and tissue health. Average score proportions for each treatment are shown in Figure 20. Total histological score proportions (Figure 18A) were calculated from the sum of the scores for each cell type observed (Figure 18B). Significant treatment effects were observed via total histological score (ANOVA,

p=0.03). Post hoc analysis indicated significantly decreased cellular health in the 5400 µg/L treatment compared to the pooled controls (Dunnett, p=0.02).

When scores for the different cell types were viewed individually, there were significant treatment effects for EM (ANOVA, p=0.03) with a significant difference in the 5400 µg/L treatment (Dunnett, p=0.02). Epidermal mucocytes in the controls and were in fair condition with some irregularity in size and pale to dark staining mucus along with visible ciliated support cells (Figure 19A). In the low treatments, 200 µg/L and 600 µg/L, epidermal mucocytes remained in fair condition with only a slightly higher presence of hypertrophied and ruptured mucocytes in the 600 µg/L treatment. The corals in the 1000 µg/L and 5400 µg/L treatments had a moderate to severe increase in the number of hypertrophied and ruptured mucocytes, with a loss of mucocytes observed in some of the 1000 µg/L corals (Figure 19C and Figure 19E). Although not as severe as seen in the avobenzone exposure, in some instances there was full ablation of the epidermis. There were significant treatment effects for CTL (Kruskal Wallis, p=0.03) and with significant differences in the 1800 µg/L and 5400 µg/L treatments (Mann Whitney U Test, p=0.03). Control corals showed minimal to mild effects, with thinning of the epidermis over costae and up to a quarter of costae exposed (Figure 19B). This is likely an artifact of post exposure handling and fixation, considering no observations of tissue thinning or loss were seen during observations of coral condition throughout the exposure. Lower treatments did not show significant increase scores for CTL; however, approximately half of the costae were exposed in the 1800 µg/L corals (Figure 19D). Corals in the 5400 µg/L treatment showed consistent significant costal tissue loss with half to three quarters of costae exposed (Figure 19F). There were no significant effects seen in zooxanthellae in the surface body wall ($p>0.05$).

There were no significant effects seen in any of the internal cellular structures including cnidoglandular bands, epidermal mucocytes in cnidoglandular bands, mesenterial filaments, gastrodermis, or the calicodermis ($p > 0.05$).

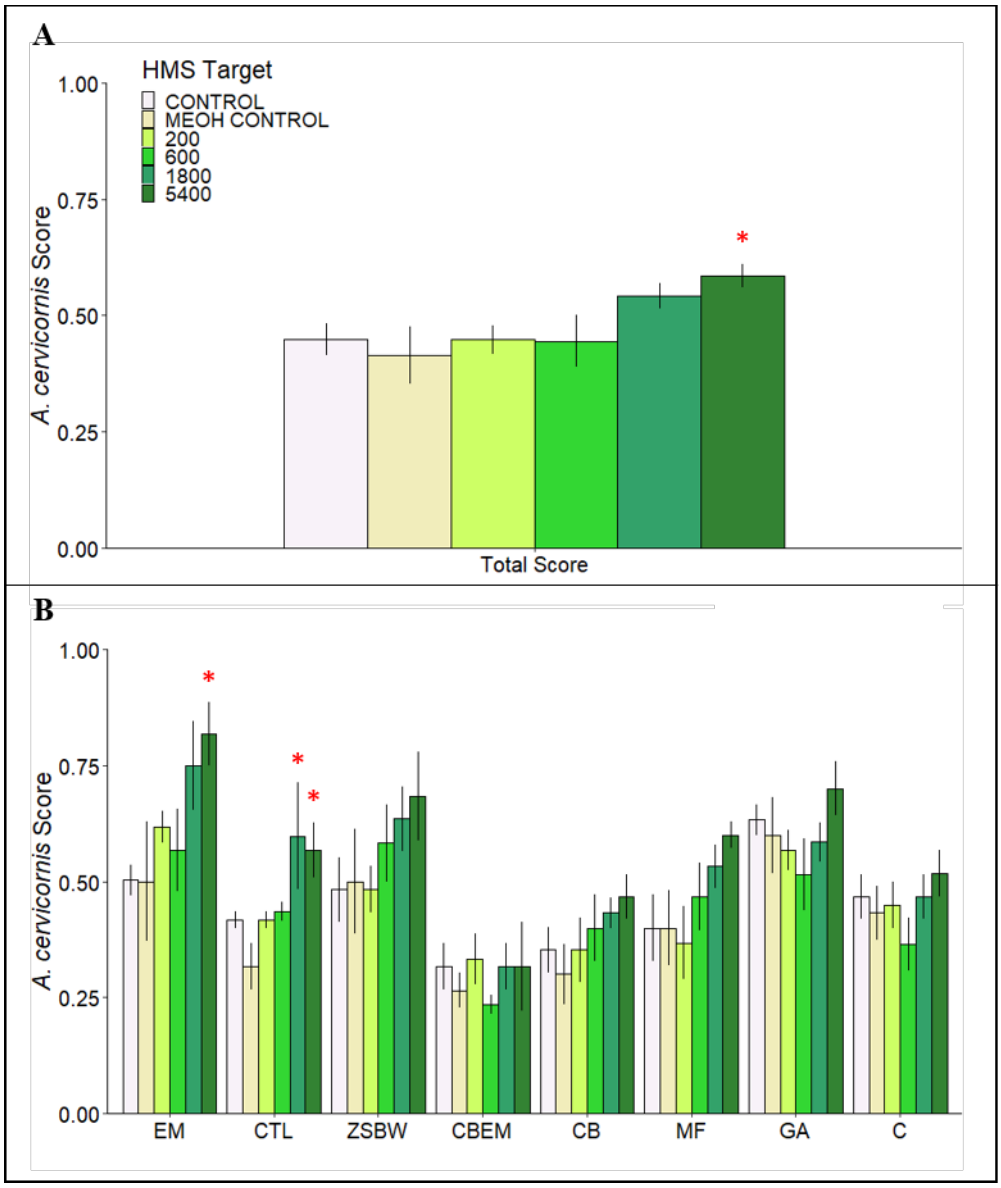

Figure 18. Mean histological score proportion (±SE) for each treatment after the 96 h homosalate exposure. (**A**) Total mean histological scores are the sums of the individually scored cell types. (**B**) Mean score proportions for each of the cell types observed; epidermal mucocytes (EM), costal tissue loss (CTL), zooxanthellae in the surface body wall (ZSBW), cnidoglandular band epidermal mucocytes (CBEM), cnidoglandular band degeneration (CB), cell dissociation on mesenterial filaments (MF), gastrodermal architecture (GA), and calicodermis (C). Red stars (*) denote significant differences ($p < 0.05$) from the pooled seawater and methanol controls (100 µl/L MeOH).

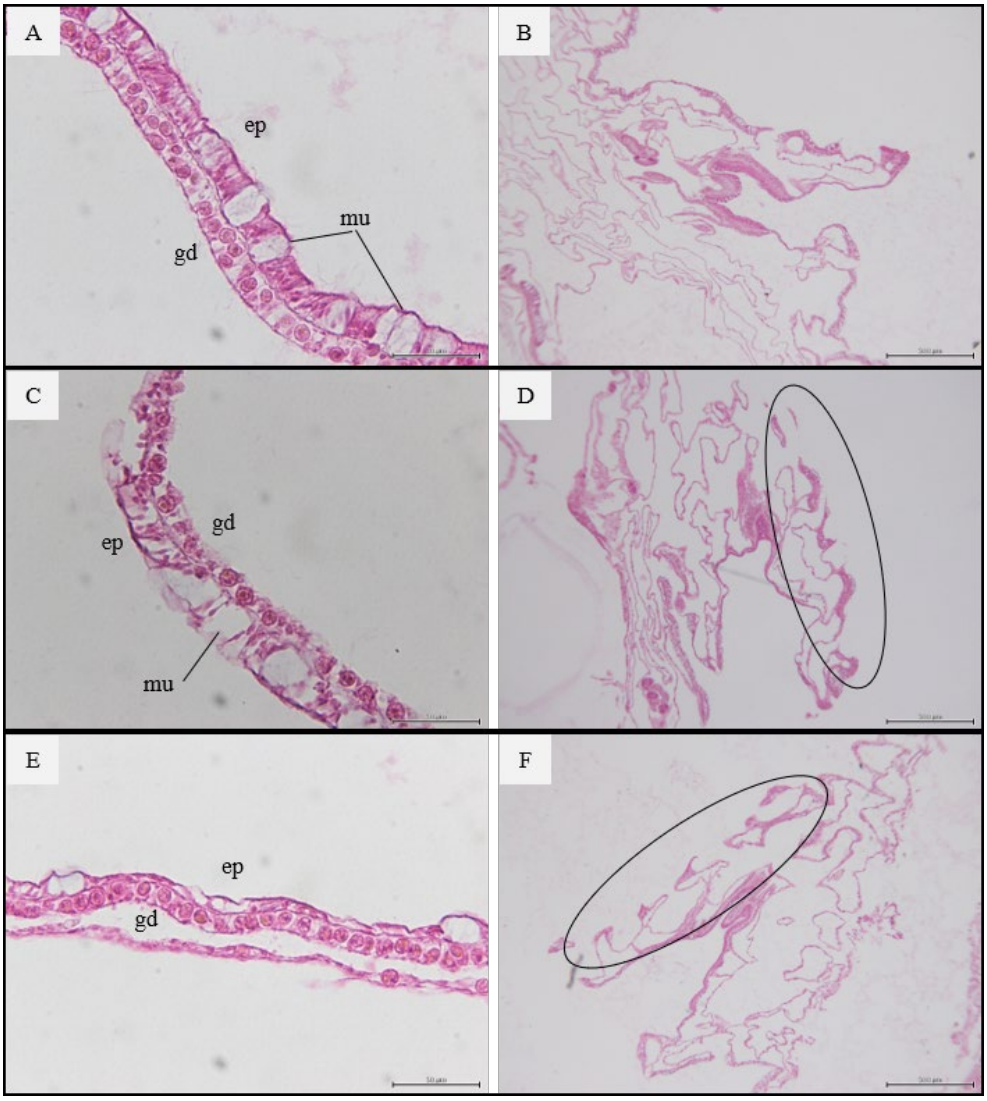

Figure 19. Histological sections of *Acropora cervicornis* surface body wall and polyps after the homosalate exposure for the seawater control and the highest two treatments. (**A**) The surface body wall and (**B**) polyp in the seawater control. (**C**) The surface body wall and (**D**) polyp in the 1800 µg/L treatment. (**E**) The surface body wall and (**F**) polyp in the 5400 µg/L treatment. Ellipses surround areas of costal tissue loss. Scale bar = 50 µm A, C, and E and 500 µm for B, D, and F. ep= epidermis, gd= gastrodermis, mu= mucocytes.

Toxicity thresholds

Effect concentrations were calculated using 10% effect concentrations (EC10) instead of EC50 due to moderate effects. A summary of all toxicity thresholds following the 96 h exposure to homosalate are summarized in Table 8.

Table 8: Effect concentrations (µg/L) after 96 h homosalate exposure. ns= not significant.

Coral Health	NOEC	LOEC	10% Effect Concentrations	95% Confidence Interval
Coral Condition	200	600	EC10: 629.9	-26.2 - 1286.1
Photosynthetic Efficiency	>5400	ns	ns	ns
Growth	>5400	ns	ns	ns
Cellular Tissue Health	1800	5400	ns	ns
Epidermal Mucocytes	1800	5400	ns	ns
Costal Tissue Loss	600	1800	ns	ns
Mortality	1800	5400	LC10: 5601.8	3615.4 - 7588.3

Sublethal (coral condition) and lethal (mortality) were estimated using dose response curves for the 96 h exposure end point (Figure 20). At 96 h, coral condition score proportions produced a significant model fit ($p=0.02$) with an EC10 of 629.9 µg/L (95% CI: -26.2 - 1286.1) (Figure 20A). The coral mortality dose response curve had a significant slope ($p=0.002$) but not a significant model fit ($p>0.05$) but was still used to estimate an EC10 of 5601.8 µg/L (95% CI: 3615.4 - 7588.3) (Figure 20B).

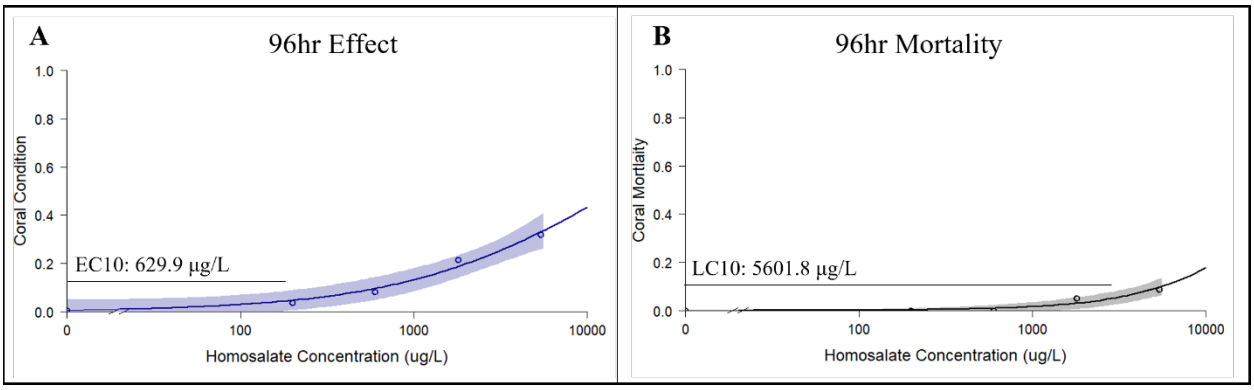

Figure 21. Homosalate dose-response curves for (**A**) coral condition score proportions and (**B**) mortality percentages at 96 h.

Sublethal inhibition thresholds were established with effects on dark-adapted maximum quantum yield and coral calcification rates (Figure 21). As there were no significant effects on yield after the 96 h exposure, there was no significant model fit and no IC50 was confirmed (Figure 21A). Also, as there were no significant effects seen in the exposure calcification rates, there was no significant model fit, as depicted in Figure 21B.

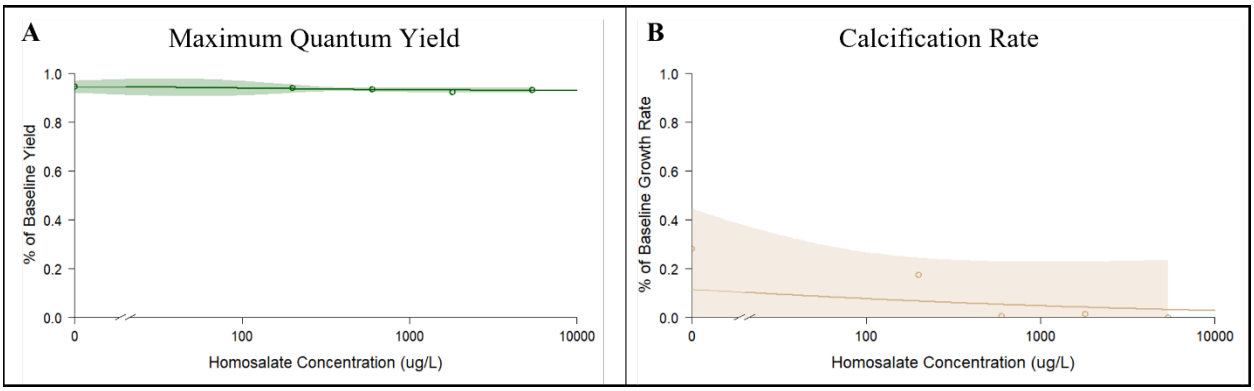

Figure 20. Homosalate dose-response curves for effects on (**A**) dark-adapted maximum quantum yield at the endpoint of the 96 h exposure and (**B**) coral calcification rates (plotted as percent of average control growth rates).

Sublethal effect thresholds were also modeled for histological parameters including total histological scores, EM, and CTL (Figure 22). None of the histological parameters produced significant model fits and no EC10s were estimated.

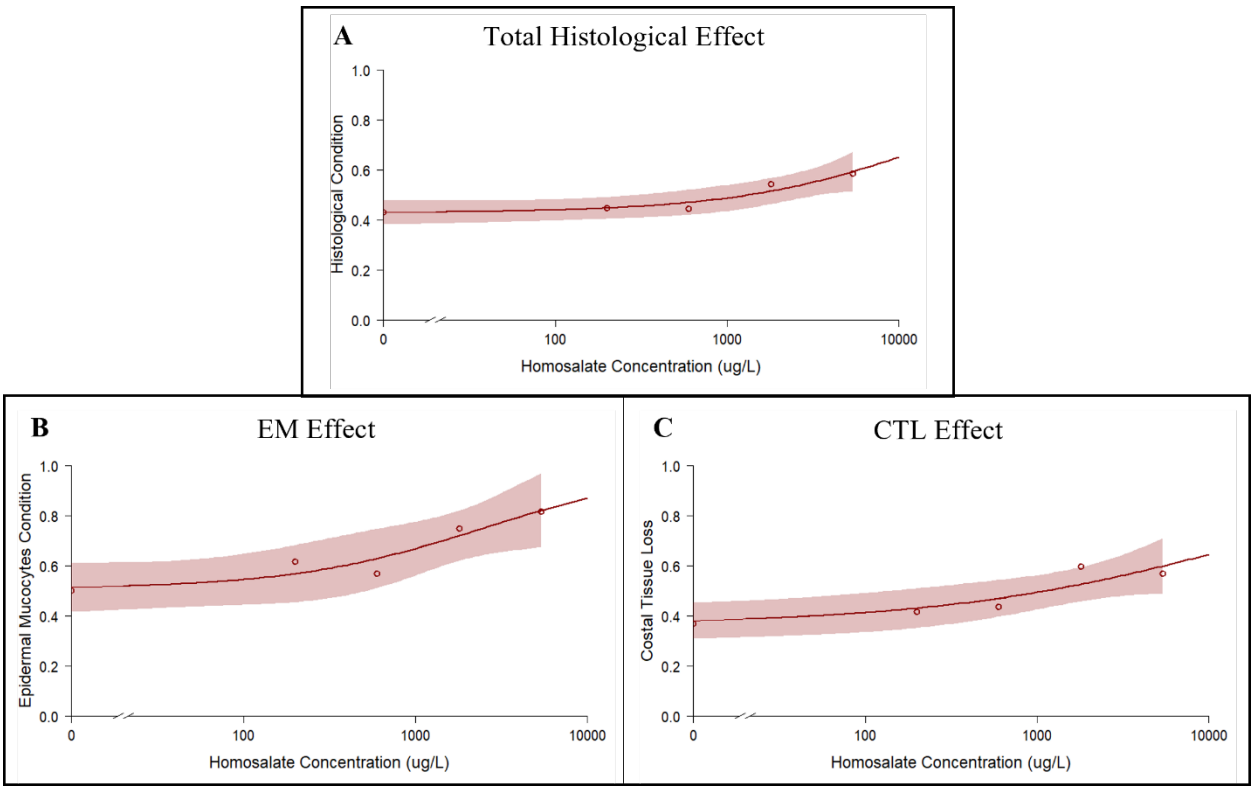

Figure 22. Homosalate dose-response curves for effects (**A**) total histological score, (**B**) epidermal mucocyte (EM) condition, and (**C**) costal tissue loss (CTL) at the endpoint of the 96 h exposure.

DISCUSSION

UV filter solubility

Avobenzone

Many organic UV filters are hydrophobic, meaning they have low water solubility and high octanol/water partition coefficients (K_{OW}). Avobenzone has a water solubility of 0.027 mg/L (27 µg/L at 20ºC) and a log K_{OW} of 6.1 (European Chemicals Agency, 2020, Mitchelmore et al. 2021). The log K_{OW} of a compound is defined as the ratio of concentration in the octanol phase to its concentration in the aqueous phase of a two-phase octanol/water system, with values typically ranging between -3 (hydrophilic) and 10 (hydrophobic) (Cumming and Rucker 2017). This signifies the equilibrium partitioning, or the likelihood of the compound to separate itself between an organic phase (e.g., sediment or coral) and an aqueous phase (e.g., seawater). With a value of 6.1, avobenzone is more likely to partition out of the water and into organic material, making reliable and consistent aquatic toxicity tests challenging. Dissolving the compound in methanol

before adding it to seawater is the standard methodology and conforms to OECD guidelines for increasing the amount of solubilized material in an aqueous phase since methanol is almost miscible in water with a log K_{OW} around -0.7 (Organisation for Economic Co-operation and Development, 2019)

The measured concentrations of avobenzone in seawater are expected to be much lower than the target nominal concentrations, as the estimated solubility of avobenzone in seawater is lower than 0.027 mg/L. Fel et al. (2019) is one of the few studies of UV filters in marine systems to provide both nominal and measured concentrations and found that measured concentrations of avobenzone in seawater were 2-22 times lower than the nominal concentrations. Nominal concentrations were 100 µg/L, 1000 µg/L, and 5000 µg/L, with measured concentrations of below level of quantification (<LOQ), 87 µg/L (± 20), and 516 µg/L (± 140), respectively. While some of these measured concentrations were well above solubility, it was predicted that the presence of a non-solubilization particulate fraction of avobenzone suspended in the water samples could have been included in the measured concentrations of the dissolved fraction. This was expected as there was no filtration of the water samples before they were analyzed. The hydrophobic nature of avobenzone is likely to lead to adherence to the sides of the glass chamber or absorption into the coral tissues, which could decrease the concentration over time. Water changes and concentration renewals were performed in this study every 24 h. However, fluctuations in the exposure level of avobenzone to the coral fragments are unavoidable in a static system.

Homosalate

The solubility of homosalate is reported at 0.5 mg/L (500 µg/L) in water (20ºC), and it has a log K_{OW} of 6.34 (European Chemicals Agency 2020, Mitchelmore et al. 2021). Homosalate has a higher solubility than avobenzone. This is likely due to the chemical structures; homosalate has one aromatic ring and one cyclohexane ring, while avobenzone has two aromatic rings. Aromatic rings reduce the solubility of compounds by lowering the ability to form hydrogen bonds. Although homosalate has a higher rate of occurrence and is commonly quantified at much higher concentrations than avobenzone (Tsui et al. 2014, Mitchelmore et al. 2019), the hydrophobic nature of homosalate provides similar challenges to maintaining consistent concentrations in laboratory exposures and measured concentrations are likely to be lower than the target nominal concentrations. As no previous studies have quantified actual exposure concentrations of

homosalate compared to expected nominal concentrations, it is difficult to predict the fate of the compound in the experimental chambers. In this study, a homosalate nominal concentration that is tenfold above solubility was used to ensure adequate exposure concentrations.

Water quality

Water quality at the end of the 96 h exposures was relatively consistent across treatments and experiments. Nutrient levels, including PO_4, NH_3, NO_2, and NO_3, showed no significant differences. Nutrient levels are likely to be higher in the presence of tissue mortality and necrosis or mucus release from stressed corals. This can be seen in some toxicity studies, such as Turner (2016) and Renegar et al. (2016), where there were higher mortality levels. While there was some mortality, particularly in the high-concentration treatments of avobenzone, it did not appear to affect nutrient levels. While there were slightly high PO_4 values in the avobenzone exposure, this was present in all chambers and therefore was likely due to contamination; possibly from washing of glassware. There were higher alkalinity values seen in both experiments in the high treatments. Alkalinity measures free ions available for calcification or coral growth. The reduction in the calcification rate observed in both experiments can account for these higher values. There were also higher pH values across treatments in both experiments. Higher pH values can result from a depletion of carbon dioxide by means of higher photosynthetic rates in stressed corals. Additionally, higher pH values can correspond to higher alkalinity values. One thing to note regarding the pH values in the high treatments of avobenzone was that, while three out of the four replicates had these higher values, the one replicate with complete mortality of both fragments showed a pH value lower than the controls, likely due to coral tissue necrosis. Lastly, in the homosalate experiment, some treatment chambers had lower dissolved oxygen values. Decreases in dissolved oxygen can often be a result elevated respiration levels in response to the higher concentrations of homosalate or higher levels of dissolved organic carbon.

Effects of avobenzone and homosalate on Acropora cervicornis

Coral condition

Avobenzone

Acropora cervicornis had a more significant stress response to avobenzone. Polyp retraction was the first sign of stress, beginning after 4 h of exposure to the three highest treatment concentrations and after 8 h to the lowest concentration. Tissue attenuation was observed after 12 h in the two highest treatments (500 µg/L and 1000 µg/L) and after 60 h in the third highest treatment (250 µg/L). There were no visible signs of bleaching, tissue swelling, or excessive mucous production throughout the exposure. There are currently no other studies to have assessed the visual effects of avobenzone on corals *ex-situ*. In Fel et al. (2019), *Stylophora pistillata* fragments showed a significant decrease in photosynthetic efficiency followed by mortality after exposure to 516 µg/L (measured concentration) avobenzone for one week. However, no observations were provided regarding sublethal visible signs of a stress response. This study's results correspond with Danovaro et al. (2008), where *Acropora sp.* exposed to 33 µg/L avobenzone for 96 h did not show significant bleaching (Danovaro et al. 2008). However, Danovaro et al. (2008) used a much lower concentration than what was used in this study, and the methodology was very different as it was modified for *in-situ* exposures.

Homosalate

Acropora cervicornis was less sensitive to homosalate compared to avobenzone. Like the avobenzone exposure, polyp retraction was the first visible stress response, starting at the very beginning of the exposure. Tissue attenuation was seen after 24 h in the highest treatment (5400 µg/L) and after 72 h in the three highest treatments (600 µg/L, 1800 µg/L, and 5400 µg/L). There were no visible signs of bleaching, tissue swelling, or excessive mucus production throughout the exposure. Stien et al. (2020) is the only study investigating homosalate effects on a coral species. A 7 d exposure of 1000 ug/L for 7 d caused polyp retraction in *Pocillopora damicornis*. However, this was the only concentration tested as this was a range finding test for metabolomic effects which were not seen.

Coral bleaching has been a common observation in studies assessing the effects of UV filters on corals (Danovaro et al. 2008, Downs et al. 2013, Downs et al. 2016, He et al. 2019a, He

et al. 2019b). Even though significant visual effects were observed in *A. cervicornis* after avobenzone and homosalate exposure, no bleaching was present. Instead, moderate to severe tissue attenuation and tissue loss was observed. Most of these previous studies use coral species such as *Pocillopora sp.* or *Stylophora sp.,* which could have varying species specific stress responses to UV filters. There could be a few explanations for the absence of bleaching in *A. cervicornis,* including species-specific stress responses or varying stress tolerances. *Acropora cervicornis* is highly susceptible to environmental factors, such as pollution, making them a suitable test species (Greer et al. 2009, Turner 2020). This sensitivity is likely the cause of the rapid progression to mortality.

Mortality

Avobenzone

Severe tissue mortality was present in *A. cervicornis* after avobenzone exposure, resulting in 100% mortality for some fragments. In the 250 µg/L treatment minimal tissue mortality was present starting at 60 h, but only resulted in 5% mortality by the end of the exposure. The two highest treatments exhibited tissue mortality starting at 24 h and progressed to as high as 85% mortality in the 500 µg/L treatment and 100% mortality in the 1000 µg/L treatment. Tissue attenuation and mortality appeared to originate around the corallites, costal ridges became more defined until the skeleton was visible, and then progressed to the coenosarc. In some cases, mortality began near the middle of the fragment and progressed to both ends, while in other cases, all corallites appeared to exhibit attenuation simultaneously. After the recovery period, there appeared to be some tissue recovery. However, it is unknown if the partially denuded coral fragments would have reached 100% recovery with more time, as the remaining fragments were fixed for histology at the 8 d post-exposure time point. Mortality results from this study correspond to results from Fel et al. (2019). Avobenzone resulted in complete mortality of *Stylophora pistillata* fragments at a measured concentration of 516 µg/L after 7 d. However, observations were made weekly, so mortality could have also been present before the 7th day. Like Fel et al. (2019), this study also showed a high percentage of mortality at the nominal concentration of 500 µg/L. However, the measured concentration is likely lower than the target nominal concentration, so it is possible that significant effects from this study could have been seen at much lower concentrations.

While there are limited studies investigating the effects of avobenzone on corals, some studies have used marine invertebrates such as *Artemia salina* and *Daphnia magna*. *Artemia salina* had significant mortality when exposed to 2000 µg/L avobenzone for 48 h (LC50 = 1840 µg/L) (Thorel et al. 2020). The toxicity of avobenzone to *Daphnia magna* has been assessed in two studies. One study estimated a LC50 of 740 µg/L in a 48 h exposure (Layton 2015). A second study assessed immobilization rates (mortality + immobility) and estimated a 48 h EC50 value of 1.95 µg/L (Park et al. 2017). Comparing these previous results to this study, it appears avobenzone had lower toxicity to *Artemia salina* compared to *Acropora cervicornis* (LC50 = 407.6 µg/L) but in some cases had higher toxicity to *Daphnia magna.*

Homosalate

Tissue mortality was less severe when *A. cervicornis* was exposed to homosalate than avobenzone. Minimal tissue mortality was present in the 1800 µg/L treatment but only resulted in 10% mortality at 96 h. The highest concentration (5400 µg/L) exhibited tissue mortality starting at 36 h and progressed to as high as 20% mortality. Similar to the avobenzone exposure, tissue attenuation and mortality appeared to originate around the corallites, but it did not reach the coenosarc. In most cases, all corallites throughout the fragment appeared to exhibit attenuation at the same time. After the 7 d post-exposure recovery, tissue mortality either appeared to remain the same or, in some cases, progress. In one fragment, tissue attenuation progressed from the corallites to parts of the coenosarc.

The toxicity of homosalate has also been evaluated in *A. salina* and *D. magna*. *Artemia salina* had significant mortality when exposed to 2000 µg/L homosalate for 48 h (LC50 = 2360 µg/L) (Thorel et al. 2020). Additionally, the toxicity of homosalate to *Daphnia magna* was assessed via acute (48 h) and chronic (21 d) exposure (Layton 2015). No significant mortality was present in the acute exposure when exposed to 600 µg/L, while the chronic exposure produced a LOEC of 600 µg/L. Comparing these results to that of homosalate and *A. cervicornis* (LC10 = 5601.8 µg/L), it appears homosalate had higher toxicity to *Artemia salina* but only a significant effect on *Daphnia magna* mortality after a chronic exposure.

Photosynthetic efficiency

Avobenzone

Photosynthetic efficiency in corals is commonly quantified in studies to monitor and predict coral bleaching via symbiont health. Reduced photosynthetic yield could signify damage to functional photosystem II (PSII), a precursor to bleaching (Hoegh-Guldberg and Jones 1999). There were no effects on the dark-adapted maximum quantum yields of the corals after exposure to avobenzone. The only comparable *ex-situ* study regarding avobenzone's effect on the photosynthetic efficiency of coral fragments observed a significant decrease in the efficiency of *S. pistillata* (Fel et al. 2019). *Stylophora pistillata* fragments exposed to 516 µg/L (measured concentration) avobenzone for 6.5 d exhibited a significantly lower yield (< 0.2), followed by mortality. There was also a significant reduction in yield when exposed to over 87 µg/L for 35 d. Measurements were taken weekly, however it is not known which week significant effects were first present, if before the final time point. This provides evidence for significant effects after chronic exposures of lower concentrations. Although no effects on the photosynthetic yield of *A. cervicornis* were seen in this study, there was significant mortality when exposed to 500 µg/L, which aligns with the Fel et al. (2019) study with *S. pistallata*. However, Fel et al. (2019) used 10 mins of dark adaptation before measurements, which is less than the recommended period of 30 mins. While it has been confirmed that most of the change in Fv/Fm occurs in the first 5- 10 mins of dark adaptation, 30 minutes of dark adaptation has been recommended as suitable for subsequent analysis of dark-adapted Fv/Fm (Hoegh-Guldberg and Jones 1999). For this study, corals were dark-adapted for 1 h to ensure accurate readings.

Unfortunately, no other studies have measured photosynthetic efficiency after avobenzone exposure. However, something of note is that avobenzone has also appears to have little to no effect on the growth of marine and freshwater algal species. Thorel et al. (2020) found no significant effect on the growth rate of *Tetraselmis sp*. at nominal concentrations as high as 1000 µg/L avobenzone, while other UV filters, including homosalate, BP-3, and OC, showed significant effects. Another study used the freshwater microalga, *Scenedesmus acutus*, and observed no significant growth inhibition effects from avobenzone at nominal concentrations as high as 9776 µg/L (Walton 2018).

Homosalate

Similar to avobenzone, there were no effects on the dark-adapted maximum quantum yields of the corals after exposure to homosalate. There are currently no other studies investigating homosalate's effect on the photosynthetic efficiency of corals or other algal species.

Interestingly, in contrast to avobenzone, evidence supports higher toxicity levels of homosalate to other marine and freshwater algal species. Homosalate was lethal to *Tetraselmis sp*. at nominal concentrations of 100 µg/L and 1 mg/L for 7 d (LC50 = 74 µg/L) (Thorel et al. 2020). The freshwater microalga, *Scenedesmus acutus*, exhibited a significant decrease in growth rates and growth inhibition from homosalate with a LOEC of 100 µg/L and a 50% inhibition (IC50) of 404 µg/L (Walton 2018). Homosalate appeared to be more toxic to *Scenedesmus* than BP-3 (LOEC 1875 = µg/L and IC50 = 1940 µg/L).

Calcification

Avobenzone

There was a significant reduction in daily growth rates of the corals in all four exposure concentrations during the avobenzone exposure. This can be supported by the water quality results, as alkalinity had significantly higher values in some of the avobenzone treatments, indicating reduced calcification rates. After 8 d of recovery, a significant difference remained between the three highest treatments and the controls. Interestingly, post-exposure growth rates in all treatments including controls, were much lower than the exposure growth rates. A possible reason for this decrease could be stress from post-exposure processing, including PAM measurements and weights, then placement into a different raceway system for recovery.

There is currently no other published work investigating the effects of organic UV filters on coral calcification rates. Only one study has observed the combined effects of BP-3 and ocean acidification on enzymes utilized in the calcification process in the yellow clam (*Amarilladesma mactroides*). They found BP-3 exposure combined with lower pH values reduced carbonic anhydrase (CA) activity in the gills of the clam (Lopes et al. 2020).

Homosalate

There were no significant treatment effects on growth rates after the 96 h exposure to homosalate. Although there appears to be reduced growth rates in the treatment groups, there were

also low values in the methanol control and overall high variability, muting any treatment effects. Negative values for growth were present in 70% of the fragments including all treatments, and both controls, indicative of a procedural error. After the 7 d recovery period, the 600 µg/L, 1800 µg/L, and the 5400 µg/L treatments were significantly lower than the controls indicating a possible post-exposure treatment effect. Only one fragment in the 600 µg/L treatment in the 7 d recovery period showed a negative value for growth.

Cellular and tissue changes

Avobenzone

Acropora cervicornis exhibited moderate to severe damage to cellular and tissue components after exposure to avobenzone. The most severe effects were seen in the surface body wall in the epidermal layer. All exposure treatments resulted in significant costal tissue loss. There was also hypertrophy and loss of epidermal mucocytes and support cells, which was significant in the three highest treatments (250 µg/L, 500 µg/L, and 1000 µg/L). The epidermal layer is the coral's first defense against pollutants and other stressors, and the mucocytes are one of the primary defense mechanisms (Brown and Bythell 2005). Increased mucus secretion has been documented with various pollutants including crude oil, copper sulfate, and mercury (Turner 2020, Mitchell & Chet 1975, Bastidas & Garcia 2004). Although no visible mucus secretion was observed in coral condition scores, it's apparent that this defense mechanism was used in the presence of organic UV filters. It has been hypothesized that mucus release can aid in the removal of pollutants. The mucus binds to the pollutant and is expelled to protect the coral (Neff and Anderson 1981, Turner 2016). In the high concentrations the higher percent mortality could be attributed to the severe mucocyte hypertrophy and full tissue ablation, which hindered the corals immune responses and defense mechanisms leaving the underlying tissues and cells exposed.

Significant effects observed in internal cellular structures were observed in the two highest treatments. Effects were present primarily in the mesenterial filaments with moderate effects to the cnidoglandular bands. While the mesenteries of the controls maintained normal structure, mesenteries in the high treatments were characterized by the increased presence of mucocytes, vacuolation, gaps in the terminal bar, and cell loss. These effects progressed to the cnidoglandular bands where there was a reduction in cells including nematocytes and granular

gland cells along with necrosis. These results are consistent with results of studies looking at effects of crude oils on coral cellular health (Peters et al. 1981, Turner 2016). The primary purpose of the mesenterial filaments is to aid in the capture and digestion of food, indicating high exposures of UV filters and other pollutants can affect the ability of the coral to heterotrophically feed. Lastly, there was a significant reduction in calicoblasts in the higher treatments. Calicoblasts assist in the formation of the skeleton by secreting an organic matrix that allows calcium carbonate crystal formation (Puverel et al. 2005, Peters, 2016). The reduction of these cells aligns with the significant reduction in growth observed, based on skeletal weight, of the corals in the high treatments.

Homosalate

Acropora cervicornis exhibited mild to moderate damage to cellular and tissue components after exposure to homosalate. The only significant effects were seen in the surface body wall in the epidermal layer. There were significant effects in the highest exposure treatment (5400 µg/L) with effects to epidermal mucocytes and support cells along with moderate costal tissue loss. The second highest treatment (1800 µg/L) also showed similar effects but with higher variability. The lower treatments remained in similar condition to the controls. Effects of homosalate on the epidermal layer were not as severe as the effects of avobenzone, suggesting either a greater ability of the coral to defend itself from this pollutant or a lesser acute effect. In contrast to the avobenzone effects, there appeared to be a slight decrease in healthy zooxanthellae in the surface body wall. Although these results were not significant this could suggest an early phase of bleaching. However, this was not supported in the results for photosynthetic efficiency. While there were no significant effects to the internal cellular structures, scores showed an increasing trend with exposure concentration in the degeneration of the cnidoglandular bands and mesenterial filaments. This could be the early phases of cellular degeneration and vacuolization, as was seen in the avobenzone exposure. Although insignificant, these results could support the need for chronic exposure testing for these and other UV filters to understand the cellular and tissue health implications to corals.

While there have been no studies to observe cellular and tissue effects of UV filters in adult corals, Downs et al. (2016) performed transmission electron microscopy (TEM) on *S. pistillata* planulae after exposure to BP-3. Similar to the above results, Downs et al. (2016) found levels of

cell death and deterioration to be more severe at the surface of the epidermis, becoming less pronounced at the center of the planulae. Observations in the epidermal layer included loss of cilia and the vacuolization and deterioration of cells (e.g., spirocysts and nematocysts). It was noted that autophagy was the dominant cellular response as none of the cells showed signs of apoptosis such as pyknosis of the nucleus. This aligns with this study as there were little to no observations of pyknotic cells but high levels of vacuolization and cell degradation.

Toxicity thresholds

Avobenzone

Toxicity thresholds for the effects of avobenzone on *A. cervicornis* were calculated based on coral condition and mortality. EC50 values decreased throughout the exposure from 653.4 µg/L at 48 h to 384.9 µg/L at 72 h to 324.4 µg/L at 96 h. LC50 values slightly decreased from 420.3 µg/L at 72 h to 407.6 µg/L at 96 h. These results suggest a time dependent effect on the toxicity of avobenzone. Endpoints for cellular effects were lower; costal tissue loss had an EC50 of 294.5 µg/L and epidermal mucocytes had an EC50 of 216.4 µg/L. Effects on growth rate had the lowest threshold value with an IC50 of 148.0 µg/L. These threshold concentrations are above the solubility of avobenzone (27 µg/L); although it is unknown at this time if the analytically confirmed concentrations remained at this level.

Corals are unlikely to experience these concentrations in the natural environment. Avobenzone has only been detected in coastal marine waters up to the ng/l level, with detection frequencies ranging from 0% to 97% (Mitchelmore et al. 2021, Tsui et al. 2014). One study performed testing of coastal water samples in eight different regions, including Hong Kong, Tokyo, Bangkok, New York, Los Angeles, Shantou, Chaozhou, and the Arctic. Avobenzone was quantified in all regions, except Chaozhou, ranging from 18 to 721 ng/L (Tsui et al. 2014). Additionally, avobenzone was quantified in South Carolina up to 597 ng/L (Bratkovics et al. 2015). However, there have been regions where avobenzone was not detected while other UV filters were. Coastal surface water testing in Hawaii found testable levels of homosalate, octisalate, and oxybenzone, while avobenzone was not detected (Mitchelmore et al. 2019).

Even though the environmental risk for *A. cervicornis* seems low based on effect concentrations determined here and real-world occurrence of avobenzone, chronic testing of lower

concentrations would be beneficial in determining the effects of extended exposures. This is especially important considering the lipophilic nature of UV filters which allows them to be retained in sediments and coral tissues. Studies have also tested sediment samples in some of the locations listed above, and avobenzone was detected at concentrations ranging from below the limits of detection (< LOD) to 64.5 ng/g (Tsui et al. 2015, Mitchelmore et al. 2019). Also, coral tissues were analyzed in Hawaii, and avobenzone was present at concentrations as high as 170 ng/g (Mitchelmore et al. 2019). Interestingly, Mitchelmore et al. (2019) found no detectable amount of avobenzone in surface water samples in Hawaii but found testable levels in both the sediments and coral tissues in the same area.

Even though results are pending for the analytical confirmation of the exposure concentrations used in this study, results from Fel et al. (2019) can be used to estimate avobenzone concentrations here. In Fel et al. (2019) the analytically confirmed concentrations were roughly 10% of the nominal concentrations; their nominal concentration of 5000 µg/L was confirmed at an average of 516 µg/L, 1000 µg/L was confirmed at an average of 87 µg/L, and 100 µg/L was confirmed to be below the limit of quantification (LOQ). If the avobenzone exposures in this study followed a similar pattern the nominal concentrations of 125 µg/L, 250 µg/L, 500 µg/L, 1000 µg/L would become 12.5 µg/L, 25 µg/L, 50 µg/L, 100 µg/L. With this consideration, toxicity thresholds would then be estimated to an EC50 of 32.45 µg/L (95% CI: 26.1 – 38.8) and an LC50 of 40.76 µg/L (95% CI: 33.1 – 48.4), which are close to the estimated solubility of avobenzone but still above concentrations found in marine environments (Tsui et al. 2015, Mitchelmore et al. 2019).

Homosalate

Effects of homosalate were not as severe as avobenzone. Accurate threshold concentrations could only be calculated at the final 96 h time point and 10% effect concentrations were used. The 96 h EC10 was 629.9 µg/L, and the LC10 of 5601.8 µg/L was higher than the tested concentration range. While the estimated solubility of homosalate (500 µg/L) is within the 95% confidence interval of the EC10 it is still well below the estimated EC50 which was greater than 5400 µg/L. As stated before, these are nominal target concentrations, and the measured concentrations are likely lower. Chronic exposure testing of homosalate would be valuable considering the proximity of the EC10 calculated in this 96 h assay to the estimated solubility.

Similar to the avobenzone results, these results are still higher than what has been quantified in coastal marine water. The highest detection recorded was in Hong Kong, where it was quantified up to 2812 ng/L (2.8 µg/L). Homosalate has additionally been quantified in Japan, New York, California, Hawaii, and the U.S. Virgin Islands, at levels ranging from 0.5 to 270 ng/L (Bargar et al. 2013, Mitchelmore et al. 2019, Tashiro et al. 2013, Tsui et al. 2014). While these values are below threshold concentrations calculated in this study, homosalate had some of the highest values recorded (>1000 ng/L) and were comparable to amounts quantified of the banned UV filters octinoxate and oxybenzone. Also, homosalate also has high detection rates, ranging from 63% to 94%. Lastly, homosalate was also quantified in sediments and coral tissues in Hawaii, ranging from 0.08 ng/g to 38.5 ng/g in sediments and 189 ng/g to 441 ng/g in coral tissues (Mitchelmore et al. 2019).

Comparative toxicology of UV filters

Comparing the results of this study to the results of other studies involving organic UV filter toxicity to corals is challenging considering the inconsistent methodology, parameters to quantify coral condition, time of exposure, coral species/life stage, and lack of calculated toxicity threshold concentrations (e.g., EC50 and LC50). There have been 11 previous studies with 9 testing individual UV filters (others used sunscreen products with multiple filters). UV filters that have been tested with corals include BP-1, BP-2, BP-3, BP-4, BP-8, EHMC, OC, EHS, 4-MBC, TDSA, octyl triazone (ET), and drometrizole trisiloxane (DT). Of these UV filters, BP-3, EHMC, OC, and 4-MBC have been banned in some regions. Coral species used include *Pocillopora damicornis, Seriatopora caliendrum, Stylophora pistillata, Acropora pulchra, and Acropora tenuis* (Mitchelmore et al. 2021). In most studies, these coral species were in the adult phase, but in 3 studies, tests were completed on coral planulae (Table A1).

Results from this study showed an avobenzone EC50 value of 324.4 µg/L, an LC50 of 407.6 µg/L, and a LOEC of 125 µg/L. Endpoint values for homosalate included an EC10 of 629.9 µg/L, LC10 of 5601.8 µg/L, and a LOEC of 600 µg/L. An avobenzone EC10 was calculated to better compare with homosalate (EC10 = 137.7 µg/L). The avobenzone EC10 and LOEC were roughly 4.5 times lower than the EC10 and LOEC of homosalate. Regarding other organic UV filters, BP-3 is one of the most studied. BP-3 has the lowest recorded EC50 value of 49 µg/L, which was estimated from the deformity of *S. pistillata* planulae (Downs et al. 2016). In the same

study, the LOEC for chlorophyll fluorescence of the planulae was 2.28 µg/L, and the LC50 was 139 µg/L. However, when looking at adult corals, He et al. (2019)a provided a 7 d LOEC of 1000 µg/L BP-3 for bleaching and mortality in *Seriatopora caliendrum* and a LOEC of 10 µg/L for polyp retraction. BP-3 was compared alongside other benzophenone UV filters using *Pocillopora damicornis* and *Seriatopora caliendrum,* and it was concluded that BP-8 and BP-1 were up to ten times more toxic to corals than BP-3, while BP-4 was the least toxic (He et al. 2019a). BP-8 was considered the most toxic, with LOECs of 100 µg/L for algal density, bleaching, and mortality in *Seriatopora caliendrum,* while the other benzophenones had LOECs of 1000 µg/L or greater.

Of the other UV filters that have demonstrated effects on corals, OC has been tested in multiple coral studies. The photosynthetic efficiency of *Stylophora pistillata* had a 35 d LOEC of 519 µg/L (measured) (Fel et al. 2019). However, another study determined 7 d LOECs of 1000 µg/L or greater for bleaching and mortality in *Pocillopora damicornis* and *Seriatopora caliendrum* (He et al. 2019b). Corals exposed to EHMC showed a similar response, with 7 d LOECs near 1000 µg/L. However, when EHMC and OC were combined, mortality LOECs dropped to 1500 µg/L EHMC and 100 µg/L OC (He et al. 2019b). The only study to investigate the effects of 4-MBC on corals is Danovaro et al. (2008), in which case *Acropora sp.* showed significant bleaching at 33 µl/L; however, *in situ* methods in this study likely had procedural effects on the coral condition, and concentrations were provided as the volume of active ingredients and not mass to volume. Based on these results, avobenzone and homosalate appear to have lower sublethal LOECs than other UV filters that have already been banned to protect reef ecosystems. Regarding lethal effect concentrations, avobenzone caused significant mortality at the concentration of 250 µg/L which is below all that of all other organic UV filters tested, except BP-8.

Inorganic, or mineral, UV filters are becoming increasingly popular as sunscreen brands strive to label their products as “reef safe.” However, studies show that these compounds also have toxic effects, primarily zinc oxide (ZnO), comparable to the effects of organic UV filters. Fel et al. (2019) found exposure of *S. pistillata* to 94 µg/L ZnO for 35 d led to a significant decrease in photosynthetic efficiency, and exposure to 864 µg/L for 14 d caused mortality. It has been suggested that exposure to ZnO can cause oxidative stress in plants and algae (Suman et al. 2015). Furthermore, ZnO can alter the symbiotic relationship between corals and their algal symbionts (Corinaldesi et al. 2018). Even in an acute 48 h exposure, ZnO caused reduced photosynthetic

efficiency and mortality in *A. cervicornis* with an estimated LC50 of 117.0 µg/L (Meurer 2022). These studies indicate that ZnO has greater acute toxicity than some organic UV filters, including avobenzone and homosalate.

CONCLUSION

This study is the first to examine the acute and subacute toxicity of the organic UV filters avobenzone and homosalate to an adult stony coral species. Due to pending results for analytically confirmed concentrations, results discussed should be viewed as nominal concentrations and it should be noted that the actual concentrations may be lower and likely varied throughout the exposure. Acute exposure to avobenzone resulted in severe stress, tissue attenuation, and mortality in *A. cervicornis*. Additional notable effects included polyp retraction, decreased growth rates, severe cellular degradation of mucocytes and epidermal tissue, and deterioration of mesenterial filaments. Although direct comparisons to other studies are not possible, these results suggest the effects of avobenzone are more severe to adult coral test species compared to other commonly banned organic UV filters. Acute exposure to homosalate resulted in moderate stress and tissue attenuation in *A. cervicornis*. Effects from acute homosalate exposure included polyp retraction and moderate cellular degradation of mucocytes and epidermal tissue. Since the effects of homosalate appeared to progress similarly to lower concentrations of avobenzone, chronic testing of homosalate is recommended to investigate how these effects may develop over time.

The low solubility of organic UV filters makes it unlikely that corals in coastal environments will be exposed to the levels used in this study. While confirmation of acute toxicity thresholds to marine organisms is valuable, more research is needed regarding the effects of chronic exposure of the lower concentrations present in coastal areas. Also, high-resolution metrics such as genetics and transcriptomics can provide more information regarding further impacts of exposure to UV filters. Lastly, future studies should analytically confirm tested UV filters' exposure concentrations and use similar metrics along with toxicity thresholds to allow accurate and comparable effect concentrations.

REFERENCES

American Cancer Society. Cancer Facts & Figures 2019. Atlanta: American Cancer Society; 2019.

Araújo, M. J., Rocha, R. J. M., Soares, A. M. V. M., Benedé, J. L., Chisvert, A., Monteiro, M. S. 2018. Effects of UV filter 4-methylbenzylidene camphor during early development of *Solea senegalensis* Kaup, 1858. Science of the Total Environment, 628-629: 1395-1404.

Balmer, M.E., Buser, H. R., Muller, M. D., Poiger, T. 2005. Occurrence of some organic UV filters in wastewater, in surface waters, and in fish from Swiss Lakes. Environ Sci Technol, 39(4): 953-962.

Barone, A.N., Hayes, C. E., Kerr, J. J., Lee1, R. C., Flaherty, D. B. 2019. Acute toxicity testing of TiO2-based vs. oxybenzone-based sunscreens on clownfish (*Amphiprion ocellaris*). Environmental Science and Pollution Research, 26: 14513–14520.

Bastidas C., Garcia E. M. 2004. Sublethal effects of mercury and its distribution in the coral *Porites astreoides*. Mar Ecol Prog Ser, 267: 133–143.

Bell, L. J., Ucharm, G., Patris, S., Diaz-Cruz, M. S., Roig, M. P. S., Dawson, M. N. 2017. Final Report Sunscreen Pollution in Jellyfish Lake. Coral Reef Research Foundation Palau.

Bock, M. 2018. Pathogen transmission techniques and genotypic resistance to disease in the threatened coral, *Acropora cervicornis*. Master's thesis. Nova Southeastern University Halmos College of Natural Sciences and Oceanography. (467)

Bratkovics, S., Wirth, E., Sapozhnikova, Y., Pennington, P., Sanger, D. 2015. Baseline monitoring of organic sunscreen compounds along South Carolina's coastal marine environment. Marine Pollution Bulletin, 101: 370–377.

Brown, B. E., Bythell J. C. 2005. Perspectives on mucus secretion in reef corals. Marine Ecology Progress Series, 296: 291-309.

Calafat, A. M., Wong, L. Y., Ye, X., Reidy, J. A., Needham, L. L. 2008. Concentrations of the Sunscreen Agent Benzophenone-3 in Residents of the United States: National Health and Nutrition Examination Survey 2003–2004. Environmental Health Perspectives, 116(7): 893–897.

Cumming, H. Rucker, C. 2017. Octanol−Water Partition Coefficient Measurement by a Simple ^{1}H NMR Method. American Chemical Society, 2: 6244-6249.

Danovaro, R., Bongiorni, L., Corinaldesi, C., Giovannelli, D., Damiani, E., Astolfi, P., Greci, L., Pusceddu, A. 2008. Sunscreens Cause Coral Bleaching by Promoting Viral Infections. Environmental Health Perspectives, 116(4): 441-447.

Da Silva, C. P., Emidio, E. S., De Marchi M. R. 2015. The occurrence of UV filters in natural and drinking water in Sao Paulo State (Brazil). Environ Sci Pollut Res Int, 22(24): 19706-19715.

Davies, P. S. 1989. Short-term growth measurements of corals using an accurate buoyant weighing technique. Marine Biology, 101: 389-395

Downs, C. A., Kramarsky-Winter, E., Fauth, J. E., Segal, R., Bronstein, O., Jeger, R., Lichtenfeld, Y., Woodley, C. M., Pennington, P., Kushmaro, A., Loya, Y. 2013. Toxicological effects of the sunscreen UV filter, benzophenone-2, on planulae and in vitro cells of the coral, Stylophora pistillata. Ecotoxicology, 23:175–191.

Downs, C. A., Kramarsky-Winter, E., Segal, R., Fauth, J., Knutson, S., Bronstein, O., Ciner, F. R., Jeger, R., Lichtenfeld, Y., Woodley, C. M., Pennington, P., Cadenas, K., Kushmaro, A., Loya, Y. 2016. Toxicopathological Effects of the Sunscreen UV Filter, Oxybenzone (Benzophenone-3), on Coral Planulae and Cultured Primary Cells and Its Environmental Contamination in Hawaii and the U.S. Virgin Islands. Arch Environ Contam Toxicol, 70: 265–288.

Du, Y., Wang, W. Q., Pei, Z. T., Ahmad, F., Xu, R. R., Zhang, Y. M., Sun, L. W. 2017. Acute Toxicity and Ecological Risk Assessment of Benzophenone-3 (BP-3) and Benzophenone-4 (BP-4) in Ultraviolet (UV)-Filters. International Journal of Environmental Research and Public Health, 14: 1-15.

European Chemicals Agency. 2020. Registered substances. Helsinki, Finland. https://echa.europa.eu/information-on-chemicals/registered-substances

Fel, J. P., Lacherez, C., Bensetra, A., Mezzache, S., Be´raud, E., Le´onard, M., Allemand, D., Ferrier-Pages, C. 2019. Photochemical response of the scleractinian coral *Stylophora pistillata* to some sunscreen ingredients. Coral Reefs, 38: 109–122.

Fent, K., Kunz, P. Y., Zenker, A., Rapp, M. 2010. A tentative environmental risk assessment of the UV-filters 3-(4-methylbenzylidene-camphor), 2-ethyl-hexyl-4-trimethoxycinnamate, benzophenone-3, benzophenone-4 and 3-benzylidene camphor. Marine Environmental Research, 69 S4-S6.

Fisher, R., O'Leary, R. A., Low-Choy, S., Mengersen, K., Knowlton, N., Brainard, R. E., Caley, M. J. 2015. Species richness on coral reefs and the pursuit of convergent global estimates. Current Biology, 25(4): 500–505.

Gago-Ferrero P., Alonso M. B., Bertozzi C. P., Marigo J., Barbosa L., Cremer M., Secchi E. R., Domit C., Azevedo A., Lailson-Brito Jr J., Torres J. P., Malm O., Eljarrat E., Díaz-Cruz M. S. 2013. First Determination of UV Filters in Marine Mammals. Octocrylene Levels in Franciscana Dolphins. Environ. Sci. Technol, 47(11): 5619–5625.

Gorham, E. D., Mohr, S. B., Garland, C. F., Chaplin, G., Garland, F. C. 2007. Do sunscreens increase risk of melanoma in populations residing at higher latitudes? Annals Epidemiol, 17: 956–963.

Greer, L., Jackson, J. E., Curran, H. A., Guilderson, T., Teneva, L. 2009. How vulnerable is *Acropora cervicornis* to environmental change? Lessons from the early to middle Holocene. Geology, 37(3): 263–266.

He, T, M. M. P. Tsui, C. J. Tan, C. Y Ma, S. K. F Yiu, L. H Wang, T. H Chen, T. Y Fan, P. K. S Lam, M. B Murphy. 2019. Toxicological effects of two organic ultraviolet filters and a related commercial sunscreen product in adult corals. Environmental Pollution, 245: 462-471. (a)

He, T, M. M. P Tsui, C. J Tan, K. Y. Ng, F. W Guo, L. H. Wang, T. H. Chen, T. Y. Fan, P. K. S. Lama, M. B. Murphy. 2019. Comparative toxicities of four benzophenone ultraviolet filters to two life stages of two coral species. Science of the Total Environment, 651: 2391–2399. (b)

Hightshoe, M. V. 2018. Identifying Disease-Resistant and Thermal-Tolerant Genotypes in the Threatened Staghorn Coral, *Acropora cervicornis.* Master's thesis. Nova Southeastern University Halmos College of Natural Sciences and Oceanography. (475)

Hoegh-Guldberg, O., Jones, R. J. 1999. Photoinhibition and photoprotection in symbiotic dinoflagellates from reef-building corals. Marine Ecology Progress Series, 183: 73-86.

Iluz, D., Dubinsky, Z. 2015. Coral photobiology: new light on old views. Science Direct, 118(2): 71-78.

Johnsen, E. C. 2018. Toxicological Effects of Commercial Sunscreens on Coral Reef Ecosystems: New Protocols for Coral Restoration. Master's capstone. Nova Southeastern University Halmos College of Natural Sciences and Oceanography. (335)

Kais B., Schneider K. E., Keiter S., Henn K., Ackermann C., Braunbeck T. 2013. DMSP modifies the permeability of the zebrafish (*Danio rerio*) chorion — Implications for the fish embryo test (FET). Aquat Toxicol, 140:229–238.

Klimova, Z., Hojerova, J., Pazourekova, S. 2013. Current problems in the use of organic UV filters to protect skin from excessive sun exposure. Acta Chimica Slovaca. no. 6(1): 82—88.

Kusk, K. O., M Avdolli, L Wollenberger. 2011. Effect Of 2,4-Dihydroxybenzophenone (BP1) on Early Life-Stage Development of the Marine Copepod *Acartia tonsa* at Different Temperatures and Salinities. Environmental Toxicology and Chemistry, 30(4): 959-966.

Layton S. M. 2015. UV filters as common organic water contaminants: a toxicological study of selected UV filters on *daphnia magna*, a monitoring study of selected Oklahoma lakes,

and the development of an undergraduate endocrine disruption authentic research lab. Doctoral dissertation. Oklahoma State University.

Lopes, F. C., de Castro, M., Barbosa S. C.,Primel, E. G., de Martinez Gaspar Martins, C. 2020. Effect of the UV filter, Benzophenone-3, on biomarkers of the yellow clam (*Amarilladesma mactroides*) under different pH conditions. Marine Pollution Bulletin, 158: 111401.

McCoshum, S. M., AM Schlarb, KA Baum. 2016. Direct and indirect effects of Sunscreen Exposure for Reef Biota. Hydrobiologia, 776: 139-146.

Miller, M. W., K. E. Lohr, C. M. Cameron, D. E. Williams, and E. C. Peters. 2014. Disease dynamics and potential mitigation among restored and wild staghorn coral, *Acropora cervicornis*. PeerJ, 2: e541.

Mitchell R., Chet I. 1975. Bacterial attack of corals in polluted water. Microb Ecol, 2: 227–233.

Mitchelmore, C. L., He, K., Gonsior, M., Hain, E., Heyes, A., Clark, C., Younger, R., Schmitt-Kopplin, P., Feerick, A., Conway, A., Blaney, L. 2019. Occurrence and distribution of UV-filters and other anthropogenic contaminants in coastal surface water, sediment, and coral tissue from Hawaii. Sci Total Environ, 670:398–410.

Moberg, F., and Folke, C. 1999. Ecological goods and services of coral reef ecosystems. Ecological Economics, 29(2):215-233.

Ngoc, L. T. N., Tran, V. V., Moon, J. Y., Chae, M., Park, D., & Lee, Y. C. 2019. Recent trends of sunscreen cosmetic: An update review. Cosmetics, 6(4), 64.

Oral, D., Erkekoğlu, P. 2020. The Safety Concerns Of Organic UV-Filters: A Special Focus On Their Endocrine Disrupting Properties. Journal of Environmental Pathology, Toxicology and Oncology, 39(3): 201–212.

Organisation for Economic Co-operation and Development. 2019. Guidance document on aquatic toxicity testing of difficult substances and mixtures. OECD Series on Testing and Assessment, No 23. ENV/JM/MONO (2000)6/REV1. Paris, France.

Park, C. B., J. Jang, S. Kim, Y. J. Kim. 2017. Single- and mixture toxicity of three organic UV-filters, ethylhexyl methoxycinnamate, octocrylene, and avobenzone on *Daphnia magna*. Ecotoxicology and Environmental Safety, 137: 57–63.

Paredes, E., S. Perez, R. Rodil, J. B. Quintana, R. Beiras. 2014. Ecotoxicological evaluation of four UV filters using marine organisms from different trophic levels *Isochrysis galbana, Mytilus galloprovincialis, Paracentrotus lividus,* and *Siriella armata.* Chemosphere, 104: 44–50.

Peters, E. C. 2016. Chapter 6: Anatomy. *Diseases of Coral*, First Edition. Edited by Cheryl M. Woodley, Craig A. Downs, Andrew W. Bruckner, James W. Porter and Sylvia B. Galloway. 2016 John Wiley & Sons, Inc. Published 2016 by John Wiley & Sons, Inc.

Peters, E. C., Meyers P. A., Yevich P. P., Blake N. J. 1981. Bioaccumulation and histopathological effects of oil on a stony coral. Marine Pollution Bulletin*,* 12(10): 333-339.

Petersen, K., H. H. Heiaas, K. E. Tollefsen. 2014. Combined effects of pharmaceuticals, personal care products, biocides and organic contaminants on the growth of *Skeletonema pseudocostatum*. Aquatic Toxicology, 150: 45–54.

Puverel, S., Tambutté, E., Zoccola, D. 2005 Antibodies against the organic matrix in scleractinians: a new tool to study coral biomineralization. Coral Reefs, 24: 149–156.

Raffa, RB, Pergolizzi, J. V., Jr., Taylor, R., Jr., Kitzen, J. M., & Group, N. R. (2019). Sunscreen Bans: Coral Reefs and Skin Cancer. Journal of Clinical Pharmacy and Therapeutics*,* 44(1), 134-139.

Reaka-Kudla, M. 1997. The global biodiversity of coral reefs: a comparison with rainforests. In: Reaka-Kudla, M., D.E. Wilson, E.O. Wilson (eds.), Biodiversity II: Understanding and Protecting our Biological Resources. Washington, D.C.: Joseph Henry Press.

Renegar, D. A., Turner, N. R. 2021. Species sensitivity assessment of five Atlantic scleractinian coral species to 1-methylnaphthalene. Scientific Reports, 11: 529.

Renegar, D. A., Turner, N. R., Riegl, B. M., Dodge, R. E., Knap, A. H., Schuler, P. A. 2016. Acute and subacute toxicity of the polycyclic aromatic hydrocarbon 1-methylnaphthalene to the shallow-water coral *porites divaricata*: application of a novel exposure protocol. Environmental Toxicology and Chemistry, 36(1): 212–219.

Richmond, R. H. (1993). Coral Reefs: Past problems and future concerns resulting from anthropogenic disturbance. Amer. Zool, 33: 524536 .

Sambandan, D. R., Ratner, D. 2011. Sunscreens: An overview and update. American Academy of Dermatology, Inc, 64 (4): 748757.

Sang, K., Leung, K. S. Y. 2016. Environmental occurrence and ecological risk assessment of organic UV filters in marine organisms from Hong Kong coastal waters. Science Direct, 566-567(1): 489-498.

Schlumpf, M., Cotton, B., Conscience, M., Haller, V., Steinmann, B., Lichtensteiger, W. 2001. In vitro and in vivo estrogenicity of UV screens. Environ Health Perspect, 109(3): 239-244.

Schneider, S. L., Lim, H. W. 2018. Review of environmental effects of oxybenzone and other sunscreen active ingredients. American Academy of Dermatology, Inc, 80(1): 266-271.

Siller, A., Blaszak, S. C., Lazar, M., Harken, O. 2019. Update About the Effects of the Sunscreen Ingredients Oxybenzone and Octinoxate on Humans and the Environment. Plastic Surgical Nursing, 38(4): 158-161.

Staberg, B., Wulf, H. C., Klemp, P., Poulsen, T., Brodthagen, H. 1983 The Carcinogenic Effect of UVA Irradiation. The Journal of Investigative Dermatology, 81: 517- 519.

Stien, D., Clergeaud, F., Rodrigues, A., Lebaron, K., Pillot, R., Romans, P., Fagervold, S., Lebaron, P. 2019. Metabolomics Reveal That Octocrylene Accumulates in *Pocillopora damicornis* Tissues as Fatty Acid Conjugates and Triggers Coral Cell Mitochondrial Dysfunction. Analytical Chemistry, American Chemical Society, 91(1): 990-995.

Tashiro, Y., Kameda, Y. 2013. Concentration of organic sun-blocking agents in seawater of beaches and coral reefs of Okinawa Island, Japan. Marine Pollution Bulletin, 77: 333–340.

Thorel, E., Clergeaud, F., Jaugeon, L., Rodrigues, A. M. S., Lucas, J., Stien, D., Lebaron, P. 2020. Effect of 10 UV Filters on the Brine Shrimp *Artemia salina* and the Marine Microalga *Tetraselmis* sp. Toxics, 8(2): 29.

Tsui M. M. P., Lam J. C. W., Ng T. Y., Ang P. O., Murphy M. B., Lam P. K.S. 2017. Occurrence, distribution, and fate of organic UV filters in coral communities. Environ Sci Technol, 51:4182–4190.

Tsui M. M. P., Leung H. W., Wai T. C., Yamashita N., Taniyasu S., Liu W., Lam P. K. S., Murphy M. B. 2014. Occurrence, distribution and ecological risk assessment of multiple classes of UV filters in surface waters from different countries. Water Res, 67:55–65.

Turner, N. 2016. Quantifying the Toxicity of 1-Methylnaphthalene to the Shallow-Water Coral, *Porites divaricata*, for Use in the Target Lipid Model. Master's thesis. Nova Southeastern University Halmos College of Natural Sciences and Oceanography. (426).

Turner, N. T. 2020. Understanding the Toxicity of Single Hydrocarbons, Oil, and Dispersed Oil: A Species Sensitivity Assessment for Five Atlantic Coral Species. Doctoral dissertation. Nova Southeastern University Halmos College of Natural Sciences and Oceanography. (533).

Vione, D., Caringella, R., Laurentiis, E., Pazzi, M., Minero, C. 2013. Phototransformation of the sunlight filter benzophenone-3 (2-hydroxy-4-methoxybenzophenone) under conditions relevant to surface waters. Science Total Environment, 463-464, 243-251.

Walton, T. 2018. Inhibition Growth Effect of Sunscreen UV Filters on the Freshwater Microalga *Scenedesmus acutus*. Honors College Thesis. Oklahoma State University. (752).

Wang, S. Q., Burnett, M. E., Lim, H. W. 2011. Safety of oxybenzone: putting numbers into perspective. Arch Dermatol, 147(7): 865-866.

Wang, S.Q., Stanfield, J,W., Osterwalder, U. 2008. In vitro assessments of UVA protection by popular sunscreens available in the United States. American Academy of Dermatology, 59(6): 934-942.

Wijgerde T., van Ballegooijen M., Nijland R., van der Loos L., Kwadijk C., Osinga R., Murk A., Slijkerman D. 2020. Adding insult to injury: Effects of chronic oxybenzone exposure and elevated temperature on two reef building corals. Sci Total Environ, 733:139030.

Williams, I., Sparks, R., Smith C. 2019. Status of Maui's coral reefs. Department of Land and Natural Resources.https://dlnr.hawaii.gov/coralreefs/files/2019/09/MauiReefDeclines.pdf

Wheate, N.J. 2022. A review of environmental contamination and potential health impacts on aquatic life from the active chemicals in sunscreen formulations. Australian Journal of Chemistry, 75(4): 241-248.

Wood, E. 2018. Impacts of Sunscreens on Coral Reefs. International Coral Reef Initiative (ICRI) Plan of Action 2016-2018.

APPENDIX

Table A1. Summary of *ex situ* studies investigating effects of UV filters on coral species.

CORAL SPECIES	UV FILTERS TESTED	CONCENTRATIONS	EXPOSURE CONDITIONS	ENDPOINTS/OBSERVATIONS	REFERENCE
Stylophora pistillata planula	BP-2	2.46 µg/L/L - 24.6 mg/L	8- 24 h (light and dark conditions)	Deformity EC20 (24 h): light 246 ng/L, dark 9.6 µg/L. LC50-light: 8hr 120 µg/L, 24 h 165 µg/L. LC50-dark: 8 h 144 µg/L, 24 h 548 µg/L	Downs et al. 2013
Stylophora pistillata cell culture	PB-2	615 ng/L to 246 mg/L	4 h (light and dark conditions)	LC50 in the light (491 µg/L) and in the dark (1.44 mg/L)	Downs et al. 2013
Stylophora pistillata planula	BP-3	228 mg/L - 2.28 µg/L/L	8- 24 h (light and dark conditions)	Deformity EC50: light 49 µg/L, dark 137 µg/L. 24 h LC50: light 139 µg/L, dark 799 µg/L	Downs et al. 2016
Stylophora pistillata cell culture	BP-3	570 ng/L - 228 mg/L	4 h (light and dark conditions)	Mortality of calicoblast cells Light: LC20 = 2 µg/L, LC50 = 42 µg/L. Dark: LC20 = 14 µg/L, LC50 = 671 µg/L	Downs et al. 2016
P. damicornis cell culture	BP-3	570 ng/L - 228 mg/L	4 h (light and dark conditions)	Mortality of calicoblast cells LC20 = 62 ng/L, LC50 = 8 µg/L/L	Downs et al. 2016
O. annularis cell culture	BP-3	570 ng/L - 228 mg/L	4 h (light and dark conditions)	Mortality of calicoblast cells LC20 = 562 ng/L, LC50 = 74 µg/L/L	Downs et al. 2016
M. cavernosa cell culture	BP-3	570 ng/L - 228 mg/L	4 h (light and dark conditions)	Mortality of calicoblast cells LC20 = 502 ng/L, LC50 = 52 µg/L/L	Downs et al. 2016
P. astreoides cell culture	BP-3	570 ng/L - 228 mg/L	4 h (light and dark conditions)	Mortality of calicoblast cells LC20 = 8 µg/L/L, LC50 = 340 µg/L/L	Downs et al. 2016
A. cervicornis cell culture	BP-3	570 ng/L - 228 mg/L	4 h (light and dark conditions)	Mortality of calicoblast cells LC20 = 63 ng/L LC50 = 9 µg/L/L	Downs et al. 2016
P. divaricata cell culture	BP-3	570 ng/L - 228 mg/L	4 h (light and dark conditions)	Mortality of calicoblast cells LC20 = 175 ng/L, LC50 = 36 µg/L/L	Downs et al. 2016
Stylophora pistillata	Avobenzone	10 - 5000 µg/L/L	5 weeks	Reduced photosynthetic efficiency LOEC = 1000 µg/L/L (87µg/L/L) and mortality LOEC = 5000 µg/L/L (measured 520 µg/L/L)	Fel et al. 2019
Stylophora pistillata	Ethylhexyl triazone (ET)	10 - 5000 µg/L/L	5 weeks	Reduced photosynthetic efficiency LOEC = 5000 µg/L/L (177 µg/L/L)	Fel et al. 2019
Stylophora pistillata	Drometrizole trisiloxane (DT)	10 - 5000 µg/L/L	5 weeks	NOEC = 5,000 µg/L/L (305)	Fel et al. 2019

Stylophora pistillata	ecamsule (TDSA)	10 - 5000 µg/L/L	5 weeks	NOEC = 5,000 µg/L/L (5,025)	Fel et al. 2019
Stylophora pistillata	Octocrylene	10 - 5000 µg/L/L	5 weeks	Reduced photosynthetic efficiency LOEC = 1,000 µg/L/L (519 µg/L/L)	Fel et al. 2019
Stylophora pistillata	ZnO	10 - 5000 µg/L/L	5 weeks	Reduced photosynthetic efficiency and mortality LOEC = 1000 µg/L/L (measured 864 µg/L/L)	Fel et al. 2019
S. caliendrum larvae	BP-1 BP-3 BP-4 BP-8	0.1 - 1000 µg/L/L	14 d	BP-1: Settlement LOEC=10 µg/L/L LC50 = 184.1 µg/L/L, bleaching LOEC= 500 BP-3: Bleaching and mortality LOEC= 1000 µg/L/L, BP-8: Settlement LOEC=10 µg/L/L LC50 = 530.1 µg/L/L, bleaching LOEC= 250, Mortality LOEC = 500 µg/L/L	He et al. 2019a
S. caliendrum adult	BP-1 BP-3 BP-4 BP-8	0.1 - 1000 µg/L/L	7 d	BP-1: Polyp retraction, algal density, bleaching, and mortality LOEC=1000 µg/L/L BP-3: Polyp retraction LOEC= 10 µg/L/L, bleaching and mortality LOEC=1000 µg/L/L BP-8: Polyp retraction LOEC= 10 µg/L/L, algal density, bleaching, and mortality LOEC=100 µg/L/L	He et al. 2019a
P. damicornis larvae	BP-1 BP-3 BP-4 BP-8	0.1 - 1000 µg/L/L	14 d	No significant effects	He et al. 2019a
P. damicornis adult	BP-1 BP-3 BP-4 BP-8	0.1 - 1000 µg/L/L	7 d	BP-1: Polyp retraction, bleaching, and mortality LOEC=1000 µg/L/L BP-8: Polyp retraction, algal density, bleaching, and mortality LOEC=1000 µg/L/L	He et al. 2019a
S. caliendrum adult	Octinoxate (EHMC) Octocrylene (OC)	0.1 - 1000µg/L/L	7 d	EHMC: Polyp retraction LOEC= 10 µg/L/L, bleaching and mortality LOEC = 1000 µg/L/L OC: Polyp retraction LOEC= 1000 µg/L/L	He et al. 2019b
P. damicornis adult	Octinoxate (EHMC) Octocrylene (OC)	0.1 - 1000µg/L/L	7 d	EHMC: Polyp retraction LOEC= 1000 µg/L/L OC: Polyp retraction LOEC= 1000 µg/L/L	He et al. 2019b
S. caliendrum adult	EHMC:OC Mix	100:5-1,500:100	7 d	Polyp retraction LOEC= 100:5 µg/L/L, Bleaching, algal density, and mortality LOEC = 1500:100 µg/L/L	He et al. 2019b
P. damicornis adult	EHMC:OC Mix	100:5-1,500:100	7 d	Polyp retraction LOEC= 400:30 µg/L/L, Bleaching, algal density, and mortality LOEC = 1500:100 µg/L/L	He et al. 2019b

P. damicornis adult	Octocrylene (OC)	5-1000 µg/L/L	7 d	Coral polyp retraction at 300 µg/L/L Abnormal fatty acid metabolism related to mitochondrial dysfunction at 50 µg/L/L	Stien et al. (2019)
P. damicornis adult	Octocrylene (OC)	5-1,000 µg/L/L	7 d	Metabolomic and mitochondrial function effect at 50 µg/L/L	Stien et al. 2020
P. damicornis adult	BP-3	5-2000 µg/L/L	7 d	Metabolomic effect at 2000 µg/L/L	Stien et al. 2020
P. damicornis adult	Octisalate (EHS)	5-1,000 µg/L/L	7 d	Metabolomic effect at 50 µg/L/L and stress/inflammatory response at 300 µg/L/L	Stien et al. 2020
P. damicornis adult	Homosalate	5-1,000 µg/L/L	7 d	Polyp retraction at 1000 µg/L/L	Stien et al. 2020
S. pistillata,	BP-3	1 µg/L (0.06 µg/L measured)	6 weeks	Microbiome changes: Increase in Verrucomicrobiaceae 4-5% decrease in PSII yield	Wijgerde et al. 2020
A. tenuis	BP-3	1 µg/L (0.06 µg/L measured)	6 weeks	5% decrease in PSII yield	Wijgerde et al. 2020

Table A2. Summary of *in situ* studies investigating effects of UV filters on coral species.

CORAL SPECIES	UV FILTERS TESTED	CONCENTRATIONS	EXPOSURE CONDITIONS	OBSERVATIONS	REFERENCE
A. divaricata, *A. cervicornis*, *A. pulchra*, *A. aspera*, *A. intermedia* adult	Octinoxate (EHMC), Octocrylene (OC), BP-3, Octisalate (EHS), Avobenzone, Enzacamene (4-MBC)	33 µL/L	96 h	Significant bleaching after exposure to EHMC, BP-3, 4-MBC. Minor to no effect from OC, EHS, and Avobenzone.	Danovaro et al. 2008
A. pluchra adult	Octinoxate (EHMC), BP-3, Enzacamene (4-MBC)	50 µL/L	96 h	Significant bleaching after exposure to EHMC, BP-3, 4-MBC.	Danovaro et al. 2008
Pocillopora spp.	Banana Boat SPF 50	4.96, 10.02, and 15.22 g/L	24 h	Bleaching occurred, but it's predicted that mere exposure caused bleaching instead of sunscreen exposure.	Skelly et al. 2012

Table A3. Histology scoring rubric modified from Miller et al. 2014 developed by Dr. Esther Peters, Megan Bock, and Morgan Hightshoe.

Parameter Viewed at 100x or 250+x, Description of "Normal"	Numerical Score Intensity or Severity Score				
0 (No Change)	**1**	**2**	**3**	**4**	**5**
High Magnification (40-60x)	**Minimal**	**Mild**	**Moderate**	**Marked**	**Severe**
Epidermal Mucocytes 0 = In 1970s sample, thin columnar cells, uniform distribution and not taller than ciliated supporting cells, pale mucus	Slightly hypertrophied, numerous, pale-staining frothy mucus. Ciliated supporting cells still very abundant.	Many cells hypertrophied, abundant release of pale staining mucus. Increase of mucus may reduce detection of columnar cells.	Uneven appearance of mucocytes, some hypertrophied but some reduced in size and secretion, darker staining mucus	Some epidermal foci lack mucocytes entirely, atrophy of epidermis and mucocytes evident, darker staining and stringy mucus, necrosis mild to minimal	Loss of many mucocytes, epidermis is atrophied to at least half of normal thickness or more, if mucus present it stains dark, thick, necrosis moderate to severe
Costal Tissue Loss 0 = Tissue covering costae intact, epidermis similar in thickness to epidermis of surface body wall with gastrodermis as it covers the costae, although this may vary with location and be thinner; calicodermis thick, pale to clear cytoplasm, or thinner with cytoplasmic extensions apically	Atrophy of epidermis, mesoglea, and calicodermis, but still intact over costae. Minimal costae exposed.	Up to one quarter of costae on corallite surfaces exposed due to loss of epithelia and mesoglea	Up to one-half of costae exposed	About three quarters of costae exposed	Most costae exposed or gaps in surface body wall present, tissues atrophied

Zooxanthellae in SBW (40-60X) 0 = Gastrodermal cells packed with well-stained algal symbionts in surface body wall, tentacles; scattered algal symbionts deeper in gastrovascular canals and absorptive cells next to mesenterial filaments	Similar to 1970s samples, thick layer of well stained algal symbionts in gastrodermis of surface body wall, tentacles, and scattered cells in gastrovascular canals and absorptive cells next to	Thick layer of well stained algal symbionts, but not quite as abundant as in 1970s samples. Mild atrophy of zooxanthellae and gastrodermis.	Algal symbionts fewer in gastrodermis which is mildly atrophied, most zooxanthellae still stain appropriately. About ½ of the zooxanthellae appear atrophied.	Single row of algal symbionts in surface body wall gastrodermis and markedly fewer in tentacle gastrodermis, some are misshapen, shrunken, or have lost acidophilic staining as proteins are no longer present or nucleus/cytoplasm has lysed, accumulation body (vacuole) enlarged compared to algal cell or missing.	No zooxanthellae present in cuboidal gastrodermal cells of colony (bleached).
Cnidoglandular Band Epithelium Mucocytes 0 = Oral portion lacks mucocytes, increasing in number aborally, may be abundant with pale mucus; difficult to assess significance of appearance	Less than half the area of cnidoglandular band is mucocytes, but could be more depending on location along the filament, size of mucocytes variable (seen in one or a few cnidoglandular bands)	About half the area is mucocytes, some hypertrophied (seen secretions in ¼ of cnidoglandular bands)	About half the area is mucocytes, all hypertrophied (seen in ½ of cnidoglandular bands)	About three quarters of the area is mucocytes, mucus production reduced, some vacuolation and necrosis present (seen in ¾ of cnidoglandular bands)	Loss of mucocytes, vacuolation and necrosis of most cells present (seen in majority of cnidoglandular bands)

Degeneration of Cnidoglandular Bands 0 = Ciliated columnar cells, nematocytes, acidophilic granular gland cells, and mucocytes abundant (but varying with location), tall, thin columnar, contiguous, terminal bar well formed	Mild reduction in cell height in one or a few areas	Cell height more reduced, mild loss of mucocytes or secretions in ¼ of cnidoglandular bands	Atrophy, loss of cells in ½ of cnidoglandular bands	Moderate atrophy of epithelium, some granular gland cells stain dark pink and are rounded, not columnar, terminal bar not contiguous, some pycnotic nuclei present, loss of cells by detachment and sloughing in ¾ of cnidoglandular bands	Severe atrophy of epithelium, detachment from mesoglea and loss of cells, necrosis or apoptosis of remaining cells, no terminal bar present, loss of cilia in majority of cnidoglandular bands
Dissociation of Cells on Mesenterial Filaments 0 = All cells intact and within normal limits, contiguous, thin columnar morphology, terminal bar present, cilia visible along apical surface	Minimal loss of cilia, but will not be present where mucocytes are predominant in one or few areas	Minimal to mild loss of cells, terminal bar has minute gaps indicating loss of ciliated cells in ¼ of mesenterial filaments	Atrophy of cells, vacuolation, reduced cilia, but filament still intact in ½ of mesenterial filaments	Rounding up and loss of granular gland cells, some pycnotic nuclei present, cell loss evident, terminal bar gaps, terminal web (junctions) between cells lost, starting to spread apart along cnidoglandular band in ¾ of mesenterial filaments	Marked to severe separation of cells, most necrotic with pycnotic nuclei, vacuolated, lysing and loss of mucocytes, nematocysts, granular gland cells and ciliated columnar cells in majority of mesenterial filaments
Gastrodermal Architecture (BBW) 0= Gastrodermis in BBW is uniform, no apparent swelling, scattered zooxathellae present but not as abundant as SBW (similar to 1976 controls). Thickness of gastrodermis variable based on lipid droplet formation. Swelling indicative	None to a few areas of swelling and cell lysing in gastrodermis, scattered zooxanthellae but less than controls	¼ of gastrodermis is swollen, cell lysing present, less zooxanthellae and some released into gastrovascular canals	½ of gastrodermis is swollen, few areas of necrotic tissue, zooxanthellae abundance reduced by ½ or ½ released into gastrovascular canals	¾ of gastrodermis is swelling, necrotic tissue, zooxanthellae abundance reduced by ¾ or ¾ released into gastrovascular canals	Entire BBW gastrodermis is necrotic, extreme swelling is visible, few to no zooxathellae present or majority of zooxanthellae released into gastrovascular canals

of potential intrusion, lysing, necrosis not seen.					
Calicodermis Condition 0 = Calicoblasts numerous both peripherally and internally, squamous but thick cytoplasm	Calicoblasts slightly reduced in height focally (more likely interior of colony, basal body wall) more squamous	About half of calicoblasts atrophied, loss of proteins in cytoplasm. Calicoblasts reduced in number	Most calicoblasts atrophied, fewer in number, spread out thinly on mesoglea, still cuboidal to columnar and active under surface body wall and in apical polyps	Most calicoblasts markedly atrophied, fewer in number, some separating from mesoglea	Basal and surface body wall calicoblasts severely atrophied or vacuolated, detaching and sloughing, or missing entirely from mesoglea